



Design, synthesis and the structure-activity relationship of agonists targeting on the ALDH2 catalytic tunnel



Ming-Che Cheng, Wei-Chi Lo, Yu-Wen Chang, Shoei-Sheng Lee, Chia-Chuan Chang*

School of Pharmacy, College of Medicine, National Taiwan University, Taipei 100, Taiwan, ROC

ARTICLE INFO

Keywords:

ALDH2
Aldehyde metabolism
Alda-1
ALDH2 agonist

ABSTRACT

ALDH2, a key enzyme in the alcohol metabolism process, detoxifies several kinds of toxic small molecular aldehydes, which induce severe organ damages. The development of novel Alda-1 type ALDH2 activators was mostly relied on HTS but not rational design so far. To clarify the structure-activity relationship (SAR) of the skeleton of Alda-1 analogs by synthesis of the least number of analogs, we prepared 31 Alda-1 analogs and 3 isoflavone derivatives and evaluated for their ALDH2-activating activity. Among these, the ALDH2-activating activity of mono-halogen-substituted (Cl and Br) *N*-piperonylbenzamides **3b** and **3k**, and non-aromatic amides **8a-8c**, were 1.5–2.1 folds higher than that of Alda-1 at 20 μ M. The relationship between binding affinity in computer aided molecular docking model and the ALDH2-activating activity assays were clarified as follows: for Alda-1 analogs, with the formation of halogen bonds, the enzyme-activating activity was found to follow a specific regression curve within the range between -5 kcal/mol and -4 kcal/mol. For isoflavone derivatives, the basic moiety on the B ring enhance the activating activity. These results provide a new direction of utilizing computer-aided modeling to design novel ALDH2 agonists in the future.

1. Introduction

Aldehyde dehydrogenase 2 (ALDH2) is an important enzyme involved in the metabolic process of alcohol. Ethanol is oxidized into acetaldehyde by alcohol dehydrogenase (ADH) in human liver, and ALDH2 further converted it into carboxylic acid to prevent human body from the damage caused by the elevation of acetaldehyde [1]. ALDH2 not only degrades acetaldehyde but also other endogenous and exogenous toxic aldehydes, such as acrolein, 2-furaldehyde, 4-HNE (4-hydroxynonenal) and DOPAL (3,4-Dihydroxyphenylacetaldehyde) [2-4]. ALDH2 widely present in the human body which requires high mitochondrial oxidative phosphorylation, especially in the liver, cardiovascular system and central nervous system [5].

About 560 million of Asians (nearly 8% of the total population in the world) are carrying the ALDH2*2 allele, and such metabolic defect is related to several severe diseases, such as cancers and cardiovascular diseases [6-9]. Elevated ALDH2 level resulted in the reduction of myocardial injury by increasing of oxidative stress in an animal model [10]. In the enzymatic studies, the Michaelis-Menten constant (K_M) and catalytic constant (k_{cat}) which represented the turnover efficacy of ALDH2*2 were 200-fold higher and 10-fold lower than those of wild type ALDH2, respectively [11]. According to the crystallography of mutated ALDH2, the Glu487Lys mutation of ALDH2*2 was founded to

be the primary reason leading to the dysfunctional aldehyde metabolism [12]. The side chain of residue Glu487 at the oligomerization domain formed two hydrogen bonds with Arg264 and Arg475, these interactions stabilized the dimer interface of ALDH2 and fixed the NAD^+ binding domain at a suitable position [13,14]. However, the Glu487Lys mutation made the protein dimer loss of the structural integrity and finally led to a positional disorder of α G (amino acids 247–260), which plays an important role in NAD^+ binding activity [11]. The X-ray crystallography showed the helix α G of ALDH2*2 were 3 Å shifted into the NAD^+ -binding cleft compared with the wild type ALDH2 which was the major reason that cause the functional loss of the mutated enzyme [12].

Alda-1 (*N*-piperonyl-2,6-dichlorobenzamide) was first identified as a potent ALDH2 agonist via a series of high-throughput screening (HTS) in 2008. Alda-1 alone enhanced the aldehyde oxidation about 2 folds for the wild-type ALDH2 and 10 folds for ALDH2*2 at 10 μ M, respectively [11]. In an animal study, treatment of Alda-1 reduced the infarction size by 60% in the ischemia/reperfusion (I/R) injury model [7]. Therefore, Alda-1 showed a strong potential of being a cardiovascular agent candidate [15-17]. However, the mechanisms for the activation of ALDH2 by Alda-1 are still unknown. In order to investigate the manner of Alda-1 in activating ALDH2, a co-crystal structure of Alda-1 in complex with ALDH2 and ALDH2*2 had been reported [11]. As

* Corresponding author.

E-mail address: chiachang@ntu.edu.tw (C.-C. Chang).

<https://doi.org/10.1016/j.bioorg.2020.104166>

Received 1 May 2020; Received in revised form 30 June 2020; Accepted 30 July 2020

Available online 25 August 2020

0045-2068/ © 2020 Published by Elsevier Inc.

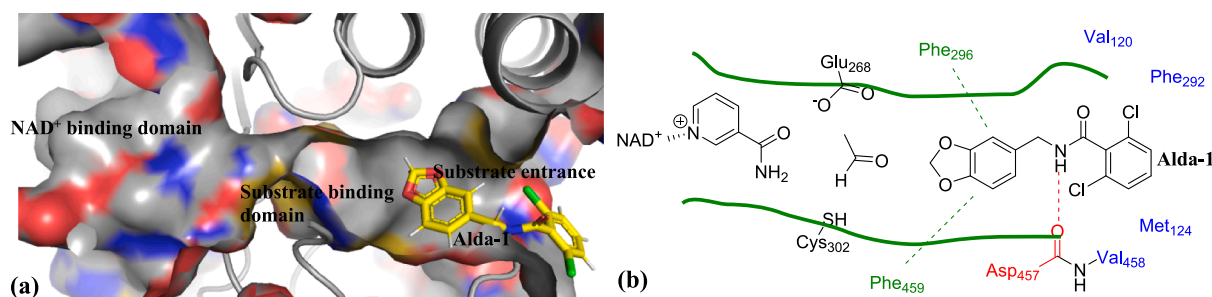


Fig. 1. (a) Alda-1 binding pose in the substrate entrance of ALDH2 (PDB ID: 3INL). (b) Important amino acid residues in the catalytic domain and the Alda-1 binding cavity of ALDH2.

shown in Fig. 1a, the catalytic domain of ALDH2 was shaped as a tunnel and could be divided into three portions, including the NAD^+ binding domain, the substrate-binding domain and the substrate entrance. The co-crystal structure also indicated that the most stable binding site of Alda-1 was located at the substrate entrance. The benzamide moiety was bounded within a hydrophobic pocket comprised of Val120, Met124, Phe292 and Val458. Inside the binding cavity, a significant hydrogen bond was formed between the amide nitrogen and the carbonyl oxygen on the main chain of Asp457. Besides, the piperonyl moiety of Alda-1 was sandwiched between Phe296 and Phe459 and were 7–8 Å apart from the catalytic triad of ALDH2 including Cys302 and Glu268 (Fig. 1b).

The X-ray crystallography of Alda-1 in complex with ALDH2 and ALDH2*2 suggested that binding with Alda-1 also lead to the conformational change of the catalytic domain. As shown in Fig. 2a, a significant shifted of αG in the apo form of ALDH2*2 (PDB code: 1ZUM) [13] was observed compared to the apo form of ALDH2 (Fig. 2b, PDB code: 3N80). However, the rotation of Phe459 in the co-crystal structure of ALDH2*2 binary complex with Alda-1 was also observed (Fig. 2c, PDB code: 3INL). The relative position of Phe296, Phe459, and the αG of ALDH2*2 binary complex with Alda-1 were highly similar with that of the apo form of ALDH2. We assumed that π - π interaction and hydrophobic interaction were the major interactions that made the aromatic side chain of Phe459 to be parallel to the piperonyl moiety of Alda-1. Such effects might be associated to the restoration of the original position of the αG helix, altered the interaction mode between ALDH2*2 and NAD^+ , and then decreased the K_M value of ALDH2*2. A plausible mechanism of action had been reported: Alda-1 enhanced the catalytic efficiency by limiting the diffusion of substrates molecules out of NAD^+ tunnel [11], it also reset the conformation of catalytic domain

back to wild-type like (i.e. ALDH2), thus enhancing the binding affinity between NAD^+ and ALDH2*2 [18].

Based on the aforementioned interaction analysis, several potent ALDH2 agonists had also been identified via HTS in the previous reports (Fig. 3) [19]. The results revealed that the *N*-benzamide scaffold had excellent potential for designing novel ALDH2 activator. However, the development of novel ALDH2 agonists were highly relied on the screening results of non-systematic-designed compounds so far, and the structure–activity relationship (SAR) of Alda-1 were not totally established. Herein, we designed and synthesized 31 *N*-benzamide derivatives based on the theoretical ligand–protein interaction analysis of Alda-1 in complex with ALDH2 and provided an exhaustive SAR analysis for a rational approach to novel ALDH2 modulator design.

2. Results and discussions

2.1. Design of Alda-1 analogs

The aforementioned computer-aided molecular docking model of protein (i.e. ALDH2, PDB code: 3INJ) in complex with 31 designed ligands (3a-3k, 6a, 6c-6g, 8a-8c, 11a-11e, 22, 24, 27a-27b, 29a-29c) had been applied to evaluate their interactions. As shown in Fig. 4, starting from the scaffold of Alda-1, the modifications on directions I to IV were focused on the B part (i.e. the benzamide moiety on the right) (direction I), the P part (i.e. the benzyl moiety on the left) (direction II), the interchange of the carbonyl positions on the linkage (direction III), and replacement of the amide linkage by non-proton donated isosteres (direction IV), respectively. The modifications on the direction I (i.e. 3a-3k) were used to verify the roles of different substituents (including halogen, methyl and hydroxy groups) on the 2 and 6 positions of B part,

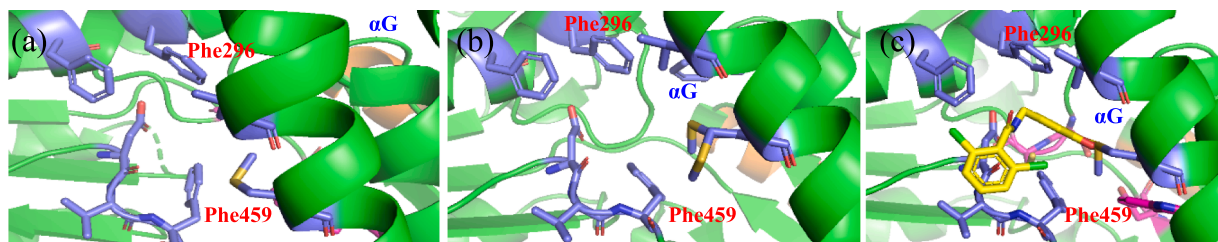


Fig. 2. Crystal structure of (a) Alda-1 binding domain of ALDH2*2, apo form (PDB code: 1ZUM) (b) Alda-1 binding domain of ALDH2, apo form (PDB code: 3N80) (c) Alda-1 binding domain of ALDH2*2 in complex with Alda-1 (PDB code: 3INL).

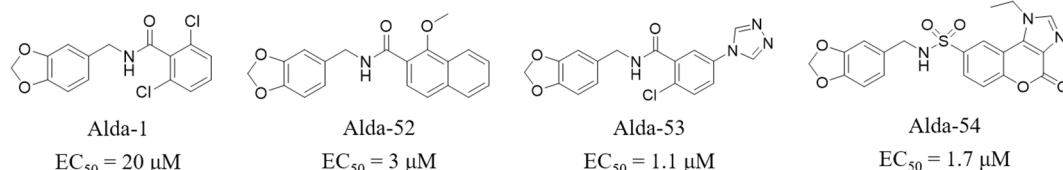


Fig. 3. Chemical structure of four reported potent ALDH2 agonists identified by high-throughput screening (HTS).

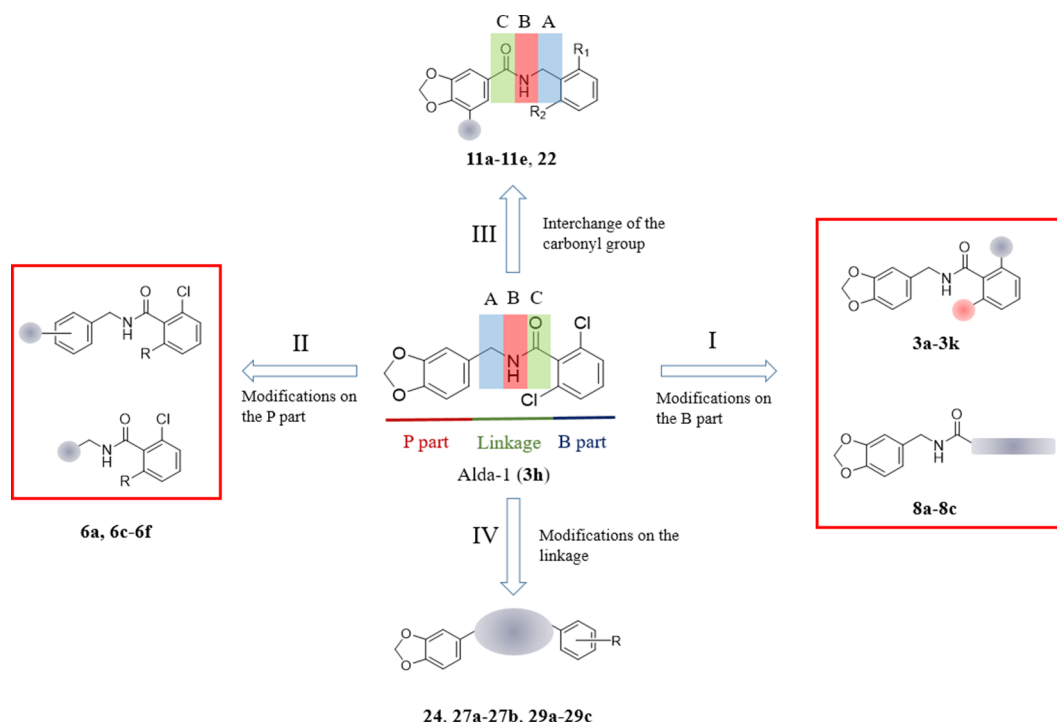


Fig. 4. Design of 31 Alda-1 analogs in directions I-IV, which were modified on the B part, P part, the position of carbonyl group and the linkage, respectively.

when interacting with the outer edge of the binding conical. In addition, to investigate the importance of the aromatic ring on the B part, the benzene ring that was replaced by three non-aromatic carbon

Table 1

Relative ALDH2-activating activity and calculated binding affinity of compounds modified on B part (**3a-3k** and **8a-8c**).

Entry	R ₁	R ₂	Activation (%) ^a	Calcd. ΔS (Kcal/mol) ^b
3a	H	H	< 10	-4.49
3b	Cl	H	67.1	-4.68
3c	I	H	< 10	-4.99
3d	Me	H	21.0	-4.61
3e	F	F	26.3	-4.95
3f	Cl	F	13.7	-4.87
3g	Cl	Me	28.8	-4.79
3i	OH	H	18.6	-4.58
3j	OH	OH	< 10	-4.67
3k	Br	H	74.3	-4.65
Alda-1 (3h)	Cl	Cl	34.8	-4.81

Entry	R	Activation rate (%) ^a	Calcd. ΔS (Kcal/mol) ^b
8a		62.0	-4.06
8b		65.3	-4.22
8c		52.0	-4.09
Alda-1 (3h)		34.8	-4.81

^a Compared with the control group (DMSO control as 0%, see Section 4.2).

^b Calculated by Molecular Operating Environment (MOE) 2008.

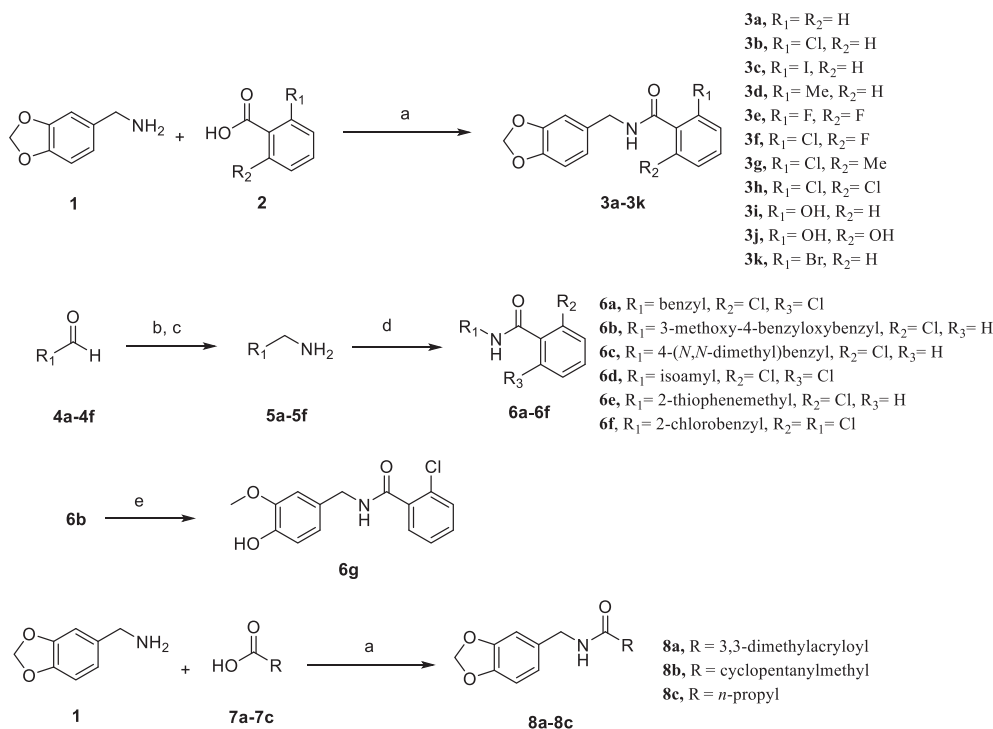
chains with 4 to 5 atoms (i.e. **8a-8c**; see Table 1) were also designed. For direction II, the piperonyl moiety (P part) was replaced by a series of aromatic and non-aromatic functional groups (**6a**, **6c-6g**; compound **6d** was replaced by non-aromatic substituent) to investigate their effects on the hydrophobic and aromatic amino acid residues in the binding site. Finally, the importance of the hydrogen bond between the ligand and Asp457 was investigated via two approaches: interchange of the carbonyl group and replacement of the amide linkage by non-hydrogen-bond-donating amide bioisosteres.

2.2. Synthesis of Alda-1 analogs

The synthetic route of compounds **3a-3k**, **6a-6g** and **8a-8c** is depicted in Scheme 1. The EDC-HOBt reaction was applied to couple various carboxylic acids with piperonyl amine to give **3a-3k** and **8a-8c**. For **6a**, **6c-6g**, primary amines **5a-5f** were prepared from the corresponding aldehydes **4a-4f** through reduction of the aldehyde oxime intermediates by zinc dust. Next, these amines were treated with arylchlorides to achieve the amide linkage of Alda-1 analogs, with total yields among 52% to 96% after purification.

For compounds **11a-11e** and **22** (see Scheme 2), protocatechuic acid (**9a**), gallic acid (**9b**) and caffeic acid (**20**) were used as the starting materials, respectively, to give the corresponding precursors (**10a-10c** and **21**). Because the phenolic hydroxy groups were unable to perform a nucleophilic attack to the dibromomethane when the carboxylic group was un-protected, the carboxyl group of **9** and **20** were protected by methyl ester via Fisher esterification before the methylenedioxy moiety was introduced. Finally, the EDC-HOBt coupling reaction was applied to condense the benzoic acid precursors with benzylamines to give the target products **11a-11e** and **22**.

In order to investigate the roles of hydrogen bonding between the ligands and Asp457, a series of non-hydrogen-bond-donating compounds, including of one ester (**24**), two tertiary amides (**27a-27b**) and three 1,2,4-oxadiazole compounds (**29a-29c**), were synthesized (see Scheme 3) (for the synthesis scheme, synthesis procedure and chemical properties of **24**, **29a** and **29b**: see p. 28–29, p. 32–33 and p. 35–36 of Supplementary Information). Next, piperonyl aldehyde **25** was



Scheme 1. Preparation of **3a-3k**, **6a-6g** and **8a-8c**. **a.** EDC-HCl, HOBT, TEA, THF, rt, 8–12 h; **b.** hydroxylamine hydrochloride, NaOAc, EtOH, rt, 12 h; **c.** zinc dust, 37% HCl_(aq), EtOH, 70 °C, 2 h; **d.** acyl chlorides, pyridine, ACN, rt, 8 h; **e.** 10% Pd/C, H₂, cat. HCl_(aq), MeOH, 24 h.

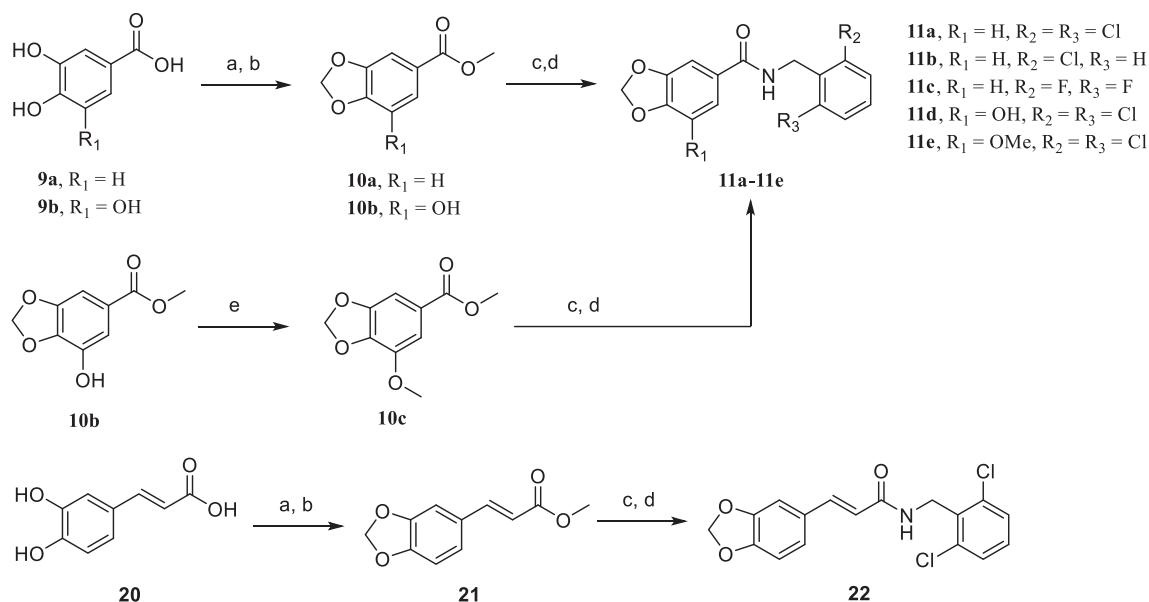
converted into amines **26a** and **26b** by reductive amination, and the two amines were further treated with 2-chlorobenzoyl chloride (prepared by Vilsmeier-Haack reaction) to give tertiary amides **27a-27b**. Finally, the end products **29a-29c** were synthesized from aldehyde **25** via two intermediates (piperonyl nitrile and amidoxime **28**), which were prepared by reported oxidative process [20] and hydroxyamination, respectively.

2.3. Design and synthesis of the isoflavone analogs

Daidzin, which was a potent natural ALDH2 inhibitors consisting of

one acidic phenolic proton, was able to bind into the same binding site as Alda-1 and inhibit the enzyme activity through blocking the entrance of the substrates [18,21,22]. The ligand-protein interaction analysis showed that the phenolic group on the ring C is proximal to Cys302 (3.8 Å) and the water molecule (3.4 Å) when binding to ALDH2 (Fig. 5a). Furthermore, ring A of daidzin were also sandwiched between Phe296 and Phe459 similar to the P part of Alda-1, and the sugar moiety (SG) formed hydrogen bond with Asp457 and Phe459 which were located at the substrate entrance (Fig. 5b).

The reported catalytic mechanism of ALDH2 included four steps (steps 1–4 in the pink region of Fig. 6), the formation of thioester bond



Scheme 2. Preparation of **11a-11e** and **22**. **a.** H₂SO₄, MeOH, reflux, 3 h; **b.** CH₂Br₂, K₂CO₃, ACN, DMF, N₂ atmosphere, 85 °C, 18 h; **c.** NaOH, H₂O, EtOH, N₂ atmosphere, 75 °C, 1.5 h; **d.** amines, EDC-HCl, HOBT, TEA, THF, rt, 8–12 h; **e.** MeI, K₂CO₃, ACN, DMF, N₂, 85 °C, 6 h.

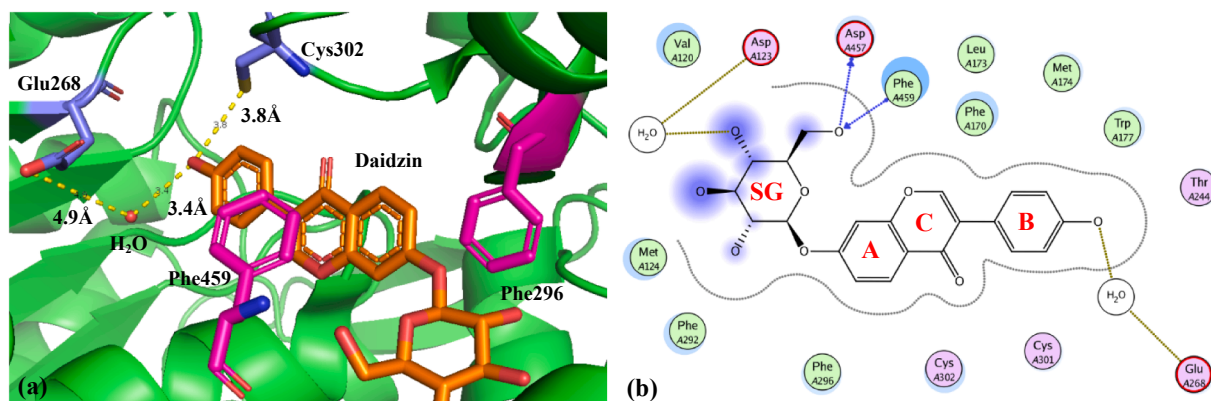
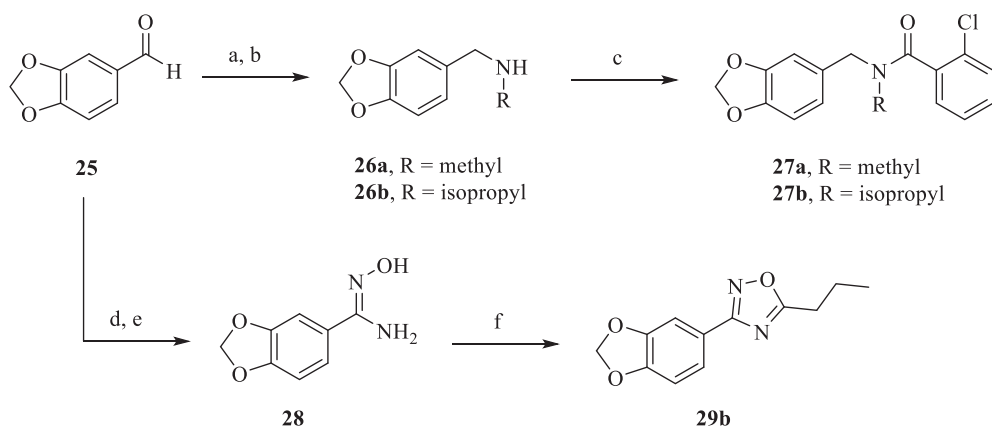


Fig. 5. (a) The docking model of ALDH2 in complex with daidzin. (b) The 2D-interaction diagram of ALDH2 in complex with daidzin, the structure of daidzin was divided into A-C ring and sugar moiety (SG).

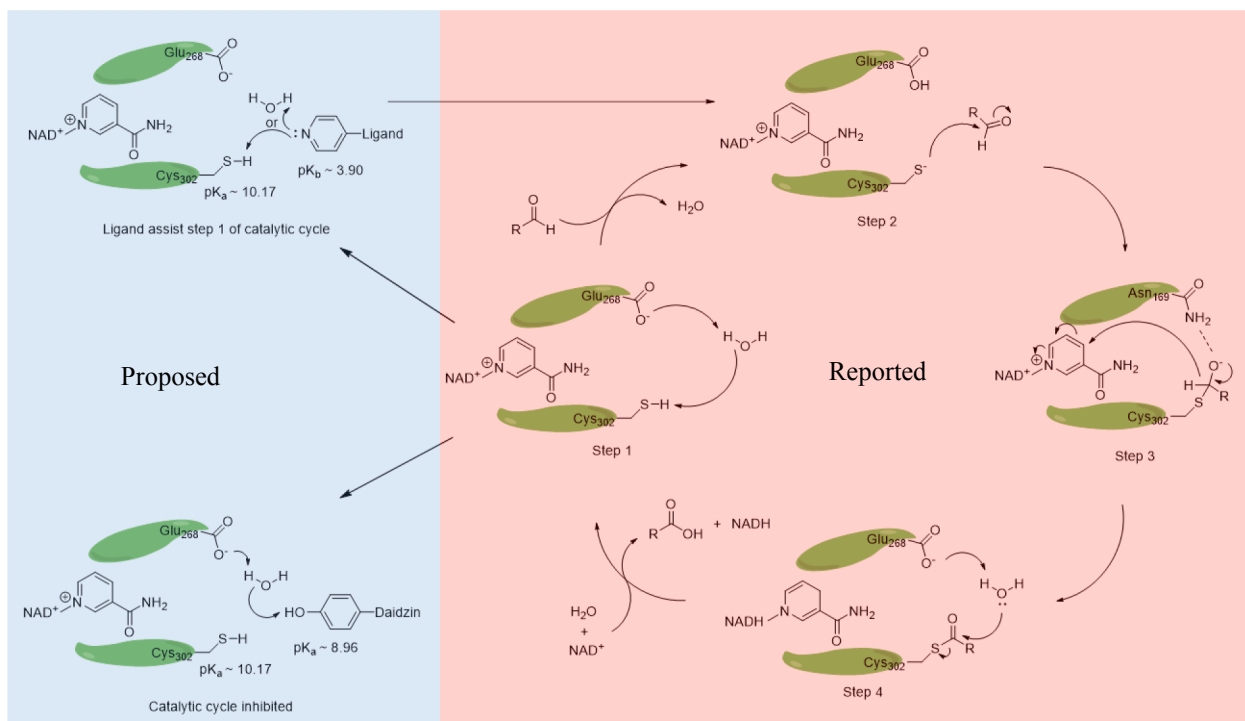


Fig. 6. The reported catalytic cycle of ALDH2 (pink region) and the proposed inhibition/activation mechanism of daidzin (**34**, calculated $pK_a \sim 8.96$) and basic isoflavone analogs **33c** (calculated $pK_b \sim 3.90$, light blue region). (For interpretation of the references to color in this figure legend, the reader is referred to the web version of this article.)

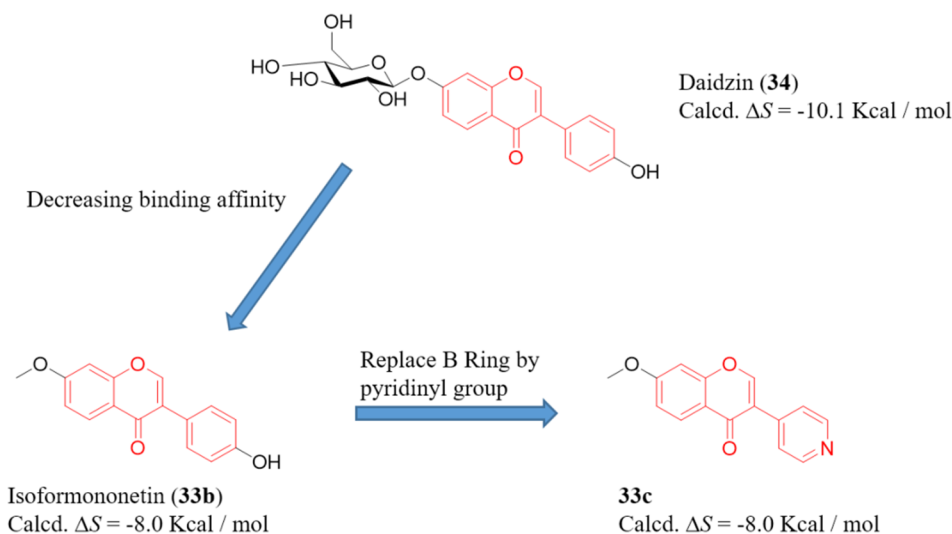
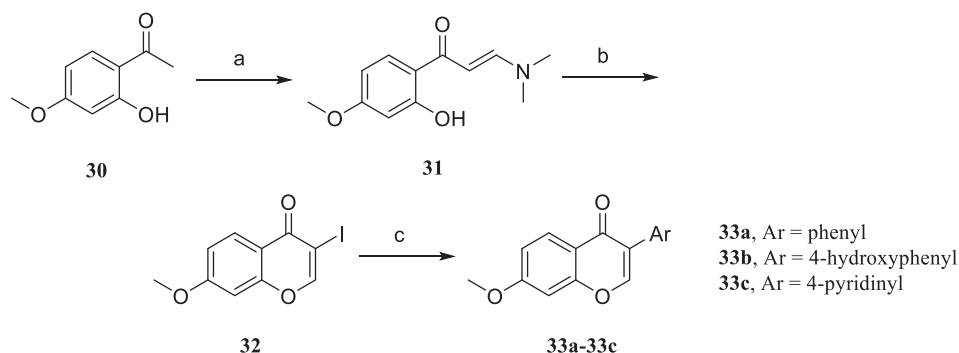


Fig. 7. Converting daidzin (**34**) from an ALDH2 inhibitor to an activator by decreasing binding affinity and modification on the ring B.

in the step 4 is important for the hydride transportation in the catalytic cycle [23], and the activation of the thiol group on Cys302 in step 1 is a key step to form the thioester intermediate. According to the simulation results, the pK_a value of the thiol group on Cys302 is 10.17 (calculated by MarvinView 20.9; 8.14 in the reference data [24]), which is closed to that of daidzin ($pK_a \sim 8.96$, calculated by MarvinView 20.9). Inspired by these studies and evidence, we assumed that daidzin could inhibit the catalytic cycle of ALDH2 not only by blocking the substrate entrance but also interrupting the proton transportation process in step 1 through donating an acidity proton to the catalytic domain. Based on this hypothesis, when the basic moiety (e.g. pyridinyl group; see the light blue region of Fig. 6) of a ligand was entering the substrate entrance and approaching Cys302, the ALDH2 activity might be enhanced by assisting the proton transportation in step 1.

Therefore, we use daidzin as a template to design and synthesis three isoflavone analogs (**33a-33c**) to investigate the effect of acidity in the catalytic center of ALDH2 (see Fig. 7). First, we replaced SG with methyl group to decrease the binding affinity of ligand. Second, the acidic substituent on ring C was replaced by basic moiety (i.e. pyridinyl group). And analog **33a** was also prepared as the neutral ligand for comparison.

The synthetic route of isoflavone analogs was depicted in Scheme 4, and the core structure of these isoflavones were synthesized by the reported methods [25]. Briefly, paeonol (**30**) was heated with dimethylformamide dimethoxyacetal (DMFDMA) to produce the enamine **31**, then cyclized the enamine moiety with hydroxyl group at meta position by iodination to give **32**. Finally, the Suzuki-Miyaura reaction was applied to couple various of arylboronic acids with **32** to give **33a-33c**.



Scheme 4. Preparation of isoflavone analogs **33a-33c**. a. DMFDMA, neat, N_2 atmosphere, 110 °C, 2 h; b. I_2 , MeOH, 60 °C, 18 h; c. arylboronic acids, $Pd(OAc)_2$, PPh_3 , K_2CO_3 , ACN, H_2O , 100 °C, 24 h.

2.4. Molecular docking analysis and biological evaluation of Alda-1 analogs

2.4.1. The in vitro evaluation results of 3a-3k and 8a-8c

The docking scores and relative ALDH2-activating activity values were listed in Tables 1-3, and the docking poses of all compounds were selected based on the binding mode of Alda-1 in the co-crystal structure (Fig. 8). In the present study, the effects of B part (see Fig. 4) was first clarified. In Alda-1, the B part is mainly composed of two chloro groups and a benzene ring. Thus in the present study, both of the two groups (i.e. the 2- and/or 6- and the benzene) were replaced by other substituents. The results for the replacement of the 2- and/or 6- substituents were shown in upper part of Table 1: compounds **3a**, **3c** and **3j** revealed no ALDH2-activating activity; the ALDH2-activating activities of **3b** and **3k** were about 1.9 and 2.1 folds stronger than Alda-1, respectively. As the results for the replacement of the benzene, as shown in lower part of Table 1, compounds **8a-8c**, in which the benzene ring of B part were replaced by acyl-groups, demonstrated ALDH2-activating activities that were 1.5–1.9 folds stronger than that of Alda-1.

2.4.2. Relationship between the formation of halogen bond and ALDH2-activating activity

The B part of the Alda-1 analogs, when docked on the active site, was located at the outer edge of the binding site, and the 2- and/or 6-halogen moiety(ies) may form halogen bonds within a specific limit distance (normally < 3.6 Å) horizontal (nucleophilic end) and vertical (electrophilic end) to the C-X bond [26]. In the docking pose of ALDH2 binary complex with Alda-1, as shown in Fig. 9a, the formation of two possible halogen bonds were observed: one was between the lone-pair

Table 2

The relative ALDH2-activating activity and calculated binding affinity of compounds modified on P part (**6a** and **6c-6g**).

Entry	R ₁	R ₂	R ₃	Activation (%) ^a	Calcd. ΔS (Kcal/mol) ^b
6a		Cl	Cl	31.1	-5.42
6c		H	Cl	25.4	-6.79
6d		Cl	Cl	16.7	-
6e		H	Cl	42.4	-4.76
6f		Cl	Cl	20.7	-6.00
6g		H	Cl	37.1	-5.06
Alda-1 (3h)		Cl	Cl	34.8	-4.81

^a Compared with the control group (DMSO control as 0%, see Section 4.2).

^b Calculated by Molecular Operating Environment (MOE) 2008.

electron of Met124 sulfur (as an electron donor; horizontal to the C-chloro A bond; calculated distance: 3.3 Å) and chloro group A, and another was the amide hydrogen on the main chain of Phe459 (as an electron acceptor; vertical to the C-chloro A bond; calculated distance: 3.5 Å). On the other side, the carbonyl group on the main chain of Tyr456 was also found to be close to the chloro group B (calculated distance: 4.4 Å). However, it was vertical to the C-chloro B bond therefore in the incorrect direction. Formation of halogen bonds in the docking results of Alda-1 and the rest 10 Alda-1 analogs (**3a-3k**) modified on the B part might be utilized to explain their percentage of activation. In Fig. 3b, the hindrance of the iodo group on the B part of **3c** lead the ligands to bind with ALDH2 in an unfavored binding pose and lose their ALDH2-activating activity. Nevertheless, the intramolecular hydrogen bond formed between the hydroxy group on the B part and the carbonyl on the linkage of **3i** and **3j** were lack of any halogen moieties to interact with Met124, Phe459 or Tyr456. Therefore, the chloro group A of Alda-1 was thought to be acted as an anchor to fix the B part at a suitable binding pose. As shown in Fig. 9c, two possible binding poses may exist, and if halogen bond between the chloro group B (Cl_B) and the carbonyl on the main chain of Tyr456 was formed, the B part would be twisted and the two important halogen bonds (with Met124 and Phe459) will disappear, and the ALDH2-activating activity will decrease. Such proposition could explain why the activation (%) of the mono-halogen-substituted analogs **3b** and **3k** (67.1% and 74.3%, respectively; see Table 1) were 1.9 folds and 2.1 folds more than di-chloro Alda-1 (34.8%), while iodo-substituted Alda-1 analog **3c** shown no ALDH2-activating activity.

2.4.3. In vitro evaluation and discussion of 6a, 6c-6 g

The results of modification on the P part were shown in Table 2. Six compounds **6a**, and **6c-6g** were synthesized. Five out of the six demonstrated similar activities with that of Alda-1, and **6d**, which was without an aromatic ring on the P part, demonstrated a weaker ALDH2-activating activity and binding affinity. These results suggested that the aromatic ring on P part was important for the ALDH2-activating activity, there presence π - π interaction between ligand, Phe296 and Phe459.

Table 3

The relative ALDH2-activating activity and calculated binding affinity of compounds modified on linkage (**11a-11e**, **22**, **27a-27b** and **29b**).

Entry	R ₁	R ₂	R ₃	Activation rate (%) ^a
11a		Cl	Cl	< 10
11b		H	Cl	< 10
11c		F	F	< 10
11d		Cl	Cl	< 10
11e		Cl	Cl	19.2
22		Cl	Cl	< 10

Entry	Linkage	R	Activation rate (%) ^a
27a			17.3
27b			< 10
29b			13.8
Alda-1 (3h)			34.8

^a **24**, **29a** and **29b** were insoluble even in 3.5% (v/v) DMSO aqueous solution, so their data were not shown.

^a Compared with the control group (DMSO control as 0%; see Section 4.2).

2.4.4. In vitro evaluation and discussion of 11a-11e, 22, 24, 27a-27b and 29a-29c

In the enzyme activation assay, the compounds which been shifted the carbonyl position (**11a-11e** and **22**) demonstrated no ALDH2-activating activity, and no meaningful molecular docking results were observed in the computer model. Following, synthesized non-hydrogen-bond-donating Alda-1 analogs (**24**, **27a-27b**, and **29a-29c**) were too lipophilic to be dissolved in 2% (v/v) DMSO aqueous solution.

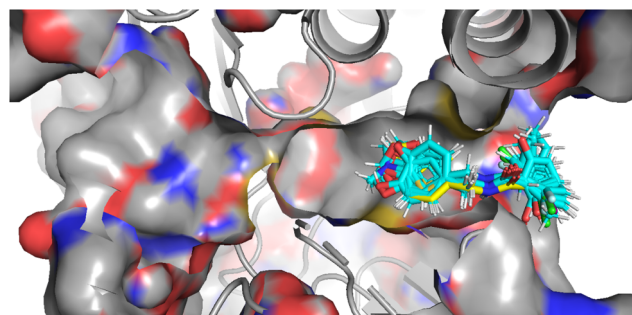


Fig. 8. Overlay of ALDH2 (PDB code: 3INL) with Alda-1 (yellow) and **3a-3k**, **6a**, **6c-6g**, **8a-8c**, **24** (light blue). (For interpretation of the references to color in this figure legend, the reader is referred to the web version of this article.)

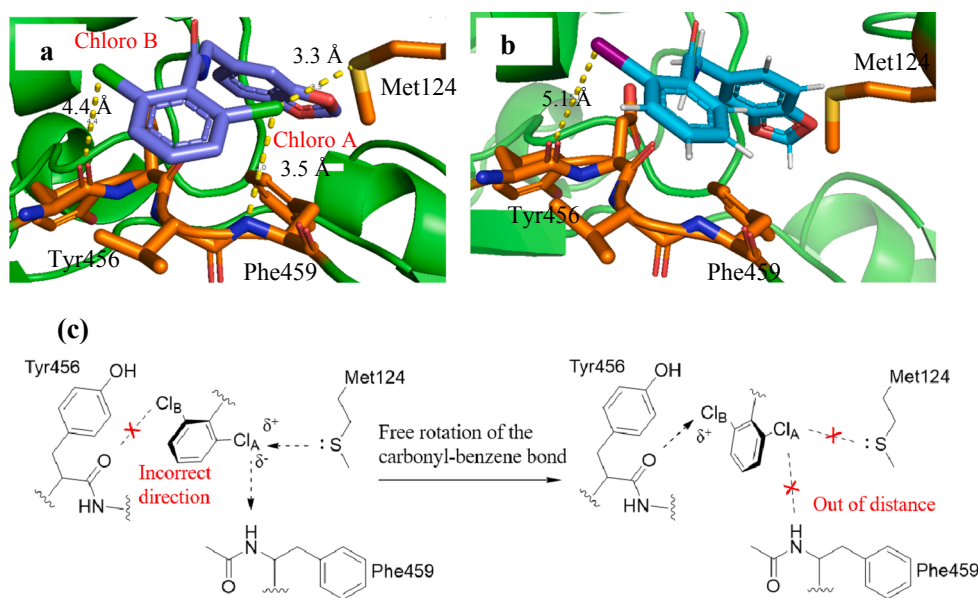


Fig. 9. (a) Binding pose of Alda-1 in the co-crystal structure, showing two halogen bonds of chloro A with Met124 and Phe459, and the distance between chloro B and carbonyl of Tyr456, which was not a halogen bond. (b) Binding pose of **3c**, showing no halogen bond formation at the outer edge of the binding site. (c) Two possible binding poses (left: Cl_B on the upper of the paper surface; right: Cl_A on the upper of the paper surface) the rotation of carbonyl-benzene bond of Alda-1, showing two (horizontal: Met124; vertical: Tyr456) and one (vertical: Phe459) halogen bonds between the B part and the indicated proximal amino acid(s), respectively.

Table 4

Isoflavone analogs and the relative ALDH2-activating activity.

Entry	Ar	R	Activation/ inhibition rate (%) ^a	Calcd. ΔS (Kcal/ mol)	Calcd. pK _a / pK _b ^b
33a		Me	7.9/-	-8.7	-/-
33b		Me	-/19.4	-8.0	8.96/-
33c		Me	22.3/-	-8.0	-/3.90
Daidzin (34)		β -Glucosyl	-/63.6	-10.1	8.96/-

^a Compared with the control group (DMSO control as 0%, see Section 4.2).

^b The pK_a values were calculated by ChemAxon-MarvinView 20.9.

Therefore, in the present study, these compounds were examined for the ALDH2-activating assay in 3% (v/v) DMSO aqueous solution. However, analogs **24**, **29a** and **29c** were dissolve poorly even in 3.5% (v/v) DMSO aqueous solution, these compounds were not able to run the *in vitro* evaluation. Beside, **27a-27b** and **29b** demonstrated weak ALDH2-activating activity. Comparing the bio-assay results of **27a-27b** and **29b** with the docking model, we surmised that the formation of the hydrogen bond between the ligand and Asp457 significantly affected the ALDH2-activating activity.

2.4.5. *In vitro* evaluation and discussion of isoflavoids 33a-33c and 34

Following the aforementioned hypothesis (see Section 2.3), the synthetic isoflavone analogs **33a-33c** were examined for their ALDH2-activating activity to validate the importance of the microenvironment in the catalytic domain of ALDH2. The molecular docking model also showed that the phenolic hydroxy group of **33a** and daidzin, and the nitrogen on the pyridinyl group of **33c** were all proximal to Cys302 with a distance around 3–4 Å. The following assay results were shown in table 4. 7-Methoxyisoflavone (**33a**) demonstrated weak activation activity toward ALDH2, and isoformononetin (**33b**) slightly inhibited

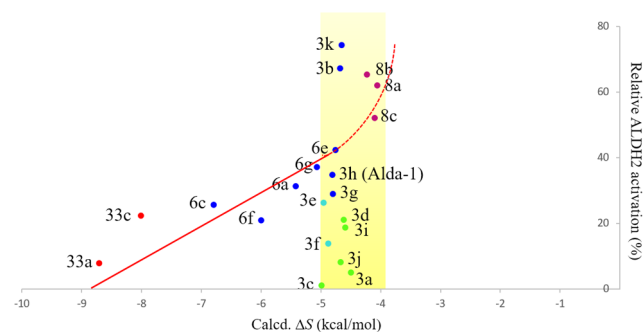


Fig. 10. Scatter plot for the calculated ΔS and the relative ALDH2 activation (%) for the 21 designed ALDH2 ligands. The suggested ΔS for ALDH2 ligands was in a range between -5 kcal/mol and -4 kcal/mol. The regression curves were linear and exponential-like in the regions lower than -5 kcal/mol and the suggested ΔS range, respectively. (Blue: Alda-1 analogs with halogen bonding formation; purple: Alda-1 analogs without aromatic ring on B part; red: isoflavone derivatives; light green: Alda-1 analogs without halogen bonding formation; light blue: Alda-1 analogs with fluoro substituents). (For interpretation of the references to color in this figure legend, the reader is referred to the web version of this article.)

the enzyme activity just like it mentioned in the previous study [27]. Surprisingly, replacement of the phenolic moiety by a pyridinyl group converted the isoflavone analogs from an inhibitor (**33b**: 19.4% inhibition) to an activator (**33c**: 22.3% activation). These results can be a powerful proof of our hypothesis and provide us a new direction for design novel ALDH2 activator.

2.4.6. Analysis of the relationship between ligands binding affinity and ALDH2-activating activity

The relationship between the calculated binding affinity (ΔS) and the relative ALDH2-activating activity (%) of the ligands was illustrated in a scatter plot, as shown in Fig. 10, and thirteen compounds were absent because of lacking calculated ΔS . Interestingly, fifteen out of twenty-one compounds were in the ΔS range between -5 kcal/mol and -4 kcal/mol. When these compounds were categorized by their structural characteristics (as the color of the dot annotated in the legends of Fig. 10), we found that non-halogen bonds formation (light green) and the compounds with fluoro group (light blue) were in the lower part of the region. In the suggested region, an exponential-like regression curve was fitted for the dots of the compounds capable of

forming halogen bonds with Met124 and Phe459; in the range lower than -5 kcal/mol, a linear regression curve was fitted. This might become the ligands with a strong binding affinity toward ALDH2 will be a blocker of the enzyme. Therefore, we suggested that binding affinity of ligands should be between -5 to -4 kcal/mol, which limited the substrate at the catalytic domain and allowed the free diffusion of the end products.

2.4.7. Structure-activity relationship of two chemical skeletons (Alda-1 and isoflavone)

Four SARs were observed: First, the B part should contain at least one chloro, or bromo group on ortho positions to form halogen bond with Met124 and Phe459, and the mono-halogen-substituted analogs revealed a stronger ALDH2-activating activity than that of Alda-1 (except **3c**, which demonstrated no activity). Second, the suggested binding affinity for ligands was in the range between -5 kcal/mol and -4 kcal/mol. Third, the aromatic moieties on P part that capable to interacting with the side chain of Phe296 and Phe459 were important for activating ALDH2 activity [although in the case absent of an aromatic ring in the P part, only one compound (**6d**) was prepared], and the amide linkage that formed hydrogen bond with Asp457 was essential for the ALDH2 agonists. Finally, the basic moiety that proximal to Cys302 of the catalytic triad (about $3-4$ Å) assisted the hydrogen transportation process and enhance the ALDH2-activating activity.

3. Conclusion

Thirty-one Alda-1 analogs and three isoflavone derivatives were prepared in the four aforementioned directions and tested for their *in vitro* ALDH2-activating activity. Four Alda-1 analogs (**3b**, **3k** and **8a-8c**) were found to have higher activities than Alda-1. Further investigations on the SAR of the two types of skeletons (Alda-1 and isoflavone) clarified the importance of a specific range of the calculated binding affinity in the computer-aided molecular docking, the proposed formation of halogen bond(s), and the basic moiety on the B ring of isoflavone derivatives. In conclusion, the SAR for Alda-1 type ALDH2 agonists was established, and these results may provide new directions for the design of novel ALDH2 agonists in the future.

4. General experiment

4.1. 3D computer docking model of the ALDH2 modulators

Crystal structure of ALDH2 (PDB ID: 3 N80), ALDH2*2 (PDB code: 1ZUM), ALDH2 bounded with Alda-1 (PDB code: 3INJ) and ALDH2*2 bounded with Alda-1 (PDB code: 3INL), were downloaded from protein data bank and modified by PyMOL 2.0.0. Small molecules were prepared and minimized the structure energy by ChemBio3D ultra. The final docking data were carried out via Molecular Operating Environment 2008 and visualized using PyMOL 2.0.0. And the chemical properties of ligands (i.e. pK_a) were calculated via MarvinView 20.9.

4.2. Assay of ALDH2-activating/inhibiting activity

The purified ALDH2 were purchased from Prospec-Tany TechnoGene Ltd. (Ness-Ziona, Israel). All the synthetic Alda-1 and isoflavone analogs were assayed for ALDH2-activating/inhibiting activity in a standard reaction mixture comprised of 100 mM tris, pH 8.0, with 0.06–0.10 μ M ALDH2, 2 mM acetaldehyde (Merck, Darmstadt, Germany), 2 mM NAD^+ (Acros, Geel, Belgium), 10 mM 2-mercaptoethanol (Sigma-Aldrich, St. Louis, MI, US), and 100 mM KCl (Showa, Tokyo, Japan). All assays were included a final concentration of 2% (v/v) DMSO (J.T. Baker, Center Valley, PA, USA) as a co-solvent and 20 μ M of sample compounds for Alda-1 analogs, and only DMSO [final concentration: 2% (v/v)] were added into the mixture for the control group. Then, all mixture was monitored at an excitation wavelength of 340 nm

at 25 °C to evaluate the initial NADH production rate of each group, and obtained the activation/inhibition rate data by compared to the control group. The enzymatic analyzed data were carried out via SpetraMax Paradigm multi-mode microplate detection platform (Molecular Device, San Jose, CA, USA).

4.3. Instrumentation and chemicals

All reagents and solvents were purchased from commercial sources including: Sigma-Aldrich, Alfa-Aesar, Merck, J.T. Baker, Fluka, Acros, and TCI chemicals. These chemicals were used without further purification. Analytical TLC was performed using aluminum plates coated with a 0.25 mm thickness of silica gel (60 F₂₅₄). Column chromatography was performed using silica gel (40–63 mesh). ¹H NMR spectra were recorded on 200 MHz (DPX-200) (Bruker, Karlsruhe, Germany) or 400 MHz (AV-400) spectrometer in CDCl₃ or methanol-*d*₄ (all signals are reported in ppm with the internal signal at 7.24 ppm for CDCl₃ and 3.30 ppm for methanol-*d*₄ as standard) at 25 °C. ¹³C NMR spectra were recorded on the same spectrometers in CDCl₃ or methanol-*d*₄ (all signals are reported in ppm with the internal signal at 77.0 ppm for CDCl₃ and 49.0 ppm for methanol-*d*₄) at 25 °C. HRMS analyses were performed on a microTOF orthogonal ESI-TOF mass spectrometer (Bruker Daltonik, Bremen, Germany). Melting points were determined by MetTemp melting point measurement apparatus (Laboratory Devices, Cambridge, MA, USA).

4.4. Chemistry

4.4.1. Procedure for synthesis of compounds **3a-3k**

To a solution of corresponding carboxylic acid (1 mmol), EDC-HCl (268.4 mg, 1.4 mmol), HOBt (189.2 mg, 1.4 mmol) and triethylamine (195 μ L, 1.4 mmol) in dry THF (5 mL) were stirred for 15 min at room temperature, and the piperonylamine (150 μ L, 1.2 mmol) was then added into the solution. The reaction mixture was stirred for 8–12 h at room temperature, and monitored by thin-layer chromatography. The resulting mixture was concentrated by reduced pressure and dissolve into EtOAc (15 mL) then partitioned by 1 N HCl aqueous solution (3×10 mL) and concentrated NaHCO₃ aqueous solution (3×10 mL), sequentially. The organic layers were dried over anhydrous MgSO₄, filtered, and concentrated under reduced pressure. The residue was recrystallized from the solution of CHCl₃-Hexane to give the amides **3a-3k**.

4.4.2. Procedure for synthesis of compounds **5a-5f**

To a solution of corresponding aldehydes (1 mmol), hydroxylamine hydrochloride (140.0 mg, 2 mmol), NaOAc (164.1 mg, 2 mmol) in EtOH (5 mL) were stirred for 12 h at room temperature. The resulting mixture was concentrated by reduced pressure and suspension in ice water, the precipitates was then filtrated and washed by ice water. Following, the precipitates were mixed with activated zinc dust (500 mg) in EtOH (5 mL), then 0.2 mL 37% HCl(aq) was added into the mixture slowly under ice bath and stirred for 2 h under 70 °C. The pH value of resulting mixture was adjusted to 8–9 by concentrated NaHCO₃ solution, then filtrated by a short pad of celite. The solution was dried over anhydrous MgSO₄, filtered, and concentrated under reduced pressure to give target amines **5a-5f**.

4.4.3. Procedure for synthesis of compounds **6a-6g**

Corresponding amines (**5a-5f**) (0.5 mmol) and pyridine (1 mL) were mixed in dry ACN (5 mL) under ice bath. The prepared acyl chlorides were then added into the mixture and stirred for 8 h at room temperature. The resulting mixture was concentrated by reduced pressure and dissolve into EtOAc (15 mL) then partitioned by 1 N HCl aqueous solution (3×10 mL) and concentrated NaHCO₃ aqueous solution (3×10 mL), sequentially. The organic layers were dried over anhydrous MgSO₄, filtered, and concentrated under reduced pressure. The

residue was purified by silica gel column chromatography (CHCl₃:MeOH from 100:0 to 75:25) to give target amides **6a-6f**. And **6b** was further stirred with 10% Pd/C and catalytic amount of 37% HCl_(aq) under H₂ atmosphere for 24 h to give the final product **6f**.

4.4.4. Procedure for synthesis of compounds **10a-10c** and **21**

To a solution of corresponding phenolic compounds (**9a-9b** and **20**) (2 mmol) and catalytic amount of concentrated sulfuric acid in MeOH (5 mL) were refluxed for 3 h. And the reaction mixture was concentrated by reduced pressure and the residue were recrystallized by MeOH. Following, the result crystals were mixed with CH₂Br₂ (174 μL, 2.5 mmol), K₂CO₃ (276.8 mg, 2 mmol) and DMF (0.5 mL) in ACN (5 mL) under N₂ atmosphere. The mixture was then heated to 85 °C and stirred for 18 h. After cooling down, the resulting mixture was concentrated by reduced pressure and purified by silica gel column chromatography (hexane:EtOAc from 85:15 to 60:40) to give target compounds **10a-10b** and **21**.

The purified compound **10b** (1 mmol) was then stirred with MeI (124.5 μL, 2.0 mmol), K₂CO₃ (276.8 mg, 2 mmol) and DMF (0.5 mL) in ACN (5 mL) under inert atmosphere. Following, the mixture was then heated to 85 °C and stirred for 6 h. After cooling down, the resulting mixture was concentrated by reduced pressure and suspension in ice water, the precipitates were then filtrated and recrystallized by CHCl₃-Hexane to give compound **10c**.

4.4.5. General procedure for synthesis of compounds **11a-11e** and **22**

Corresponding compounds (**10a-10c** and **21**) (0.8 mmol) were dissolved in EtOH (0.5 mL) and NaOH aqueous solution (pH 10.0, 4.5 mL) was added to the mixture and heated to 75 °C under N₂ atmosphere for 1.5 h. After cooling down, the pH value of reaction mixture was adjusted to 5–6 by 1 N HCl aqueous solution. 10 mL of distilled water was then added to the resulting mixture and partitioned with EtOAc (3 × 10 mL). Combined the organic layers, dried over anhydrous MgSO₄, filtered, and concentrated under reduced pressure. Following, the solution of resulting solid, EDC-HCl (268.4 mg, 1.4 mmol), HOBT (189.2 mg, 1.4 mmol) and triethylamine (195 μL, 1.4 mmol) in dry THF (5 mL) were stirred for 15 min at room temperature, and the benzylamines (1 mmol; prepared by the procedure shown in Section 4.4.2) was then slowly added into the solution. The reaction mixture was stirred for 8–12 h at room temperature, and monitored by thin-layer chromatography. The resulting mixture was concentrated by reduced pressure and dissolve into EtOAc (15 mL) then partitioned by 1 N HCl aqueous solution (3 × 10 mL) and concentrated NaHCO₃ aqueous solution (3 × 10 mL), sequentially. The organic layers were dried over anhydrous MgSO₄, filtered, and concentrated under reduced pressure. The residue was recrystallized from the solution of CHCl₃-Hex to give target amides **11a-11e** and **22**.

4.4.6. Procedure for synthesis of compounds **26a-26b**

To a solution of piperonyl aldehyde (2 mmol), corresponding amine hydrochlorides (3 mmol) and triethylamine (3 mmol) in THF (8 mL) were stir at 50 °C for 4 h. Following, 10% Pd/C was added into the reaction mixture and stir under H₂ atmosphere at room temperature for 12 h. The resulting mixture was concentrated by reduced pressure and purified by silica gel column chromatography (CHCl₃:MeOH from 100:0 to 75:25) to give target amines **26a-26b**.

4.4.7. Procedure for synthesis of compounds **27a-27b**

Corresponding amines (**26a-26b**) (1 mmol) and pyridine (1 mL) were mixed in dry ACN (5 mL) under ice bath. The prepared acyl chlorides were then added into the mixture and stirred for 24 h at room temperature. The resulting mixture was concentrated by reduced pressure and purified by silica gel column chromatography (CHCl₃:MeOH from 100:0 to 50:50) to give target amides **27a-27b**.

4.4.8. Procedure for synthesis of compounds **29b**

To a solution of piperonyl aldehyde (2 mmol), iodine (558.4 mg, 2.2 mmol) and 28% ammonia hydroxide solution (2 mL) in ACN (4 mL) were stirred for 4 h at room temperature. The excess iodine was quenched by concentrated Na₂S₂O₃ solution, and the reaction mixture was concentrated by reduced pressure and the residue were filtrated and washed by water. Following, the residue was mixed with hydroxylamine hydrochloride (140.1 mg, 2.0 mmol), K₂CO₃ (138.5 mg, 1 mmol) and water (1.5 mL) in isopropyl alcohol (3.5 mL) and refluxed for 6 h. After cooling down, the resulting mixture was concentrated by reduced pressure and the residue were washed by water and recrystallized by acetone-hexane to give compound **28**.

Following, compound **28** (1 mmol) and pyridine (1 mL) were mixed in dry ACN (5 mL). And the prepared butyryl chloride was then added into the mixture and heated to 80 °C for 6 h. The resulting mixture was concentrated by reduced pressure and dissolve into EtOAc (15 mL) then partitioned by 1 N HCl aqueous solution (3 × 10 mL) and concentrated NaHCO₃ aqueous solution (3 × 10 mL), sequentially. The organic layers were dried over anhydrous MgSO₄, filtered, and concentrated under reduced pressure. The residue was recrystallized from the solution of CHCl₃-Hex to give target compounds **29b**.

4.4.9. Procedure for synthesis of compounds **31**

To a solution of paeonol (**30**; 336.2 mg, 2 mmol) and DMFDMA (750 μL, 5.6 mmol) were sealed in the seal flask under N₂ atmosphere and stirred at 110 °C for 2 h. After cooling down, the resulting mixture was washed by cold MeOH then recrystallized from the solution of CHCl₃-Hex to give target compounds **31**.

4.4.10. Procedure for synthesis of compounds **32**

To a solution of **31** (221.0 mg, 1 mmol), iodine (308.4 mg, 1.2 mmol) and MeOH (4 mL) were stirred at 60 °C for 18 h. The excess iodine was quenched by concentrated Na₂S₂O₃ solution, and the reaction mixture was concentrated by reduced pressure and the residue were filtrated and washed by water. The resulting residue was purified by silica gel column chromatography (CHCl₃:MeOH from 100:0 to 75:25) to give target compound **32**.

4.4.11. Procedure for synthesis of compounds **33a-33c**

To a solution of **32** (151.0 mg, 0.5 mmol), corresponding arylboronic acid (0.6 mmol), K₂CO₃ (138.2 mg, 1 mmol), PPh₃ (15.5 mg, 6 mol%), Pd(OAc)₂ (12.0 mg, 5 mol%), distilled water (2 mL) and ACN (3 mL) were sealed in the seal flask under N₂ atmosphere. The mixture was heated to 100 °C and stirred for 24 h. The pH value of resulting mixture was adjusted to 5–6 by 1 N HCl solution, then filtrated by a short pad of celite. The resulting mixture was concentrated by reduced pressure and purified by silica gel column chromatography (CHCl₃:MeOH from 100:0 to 75:25) to give target compounds **33a-33c**.

4.5. Chemical properties

4.5.1. *N*-(3,4-Methylenedioxy)benzylbenzamide (**3a**)

White solid; m.p.: 114–115 °C

IR (KBr): 3305, 3067, 3002, 2975, 2940, 2894, 2846, 2787, 1974, 1853, 1759, 1629, 1604, 1578, 1499, 1440, 1309, 1251, 1229, 1090, 1043, 940, 821, 769, 720, 697, 640 cm⁻¹

¹H NMR (400 MHz, CDCl₃) data:

δ 7.76–7.74 (m, 2H), 7.46 (tt, *J* = 7.3, 1.1 Hz, 1H), 7.38 (t, *J* = 7.2 Hz, 2H), 6.80 (d, *J* = 1.3 Hz, 1H), 6.76 (dd, *J* = 8.0, 1.4 Hz, 1H), 6.72 (d, *J* = 7.9 Hz, 1H), 6.63 (br. s, 1H, D₂O exchangeable), 5.90 (s, 2H), 4.48 (d, *J* = 5.6 Hz, 2H)

¹³C NMR (50 MHz, CDCl₃) data:

δ 167.3 (C), 147.9 (C), 146.9 (C), 134.2 (C), 132.0 (C), 131.5 (CH), 128.5 (CH), 126.9 (CH), 121.1 (CH), 108.4 (CH), 108.3 (CH), 101.0 (CH₂), 43.8 (CH₂)

HR-ESI-MS: Positive mode: calcd. For $C_{15}H_{13}NO_3Na$ (m/z): 278.0788; found: 278.0792 ($[M + Na]^+$)

4.5.2. *N*-(3,4-Methylenedioxy)benzyl-2-chlorobenzamide (3b)

White solid; m.p.: 102–103 °C

IR (KBr): 3304, 3074, 3002, 2930, 2893, 2778, 1849, 1644, 1592, 1531, 1504, 1443, 1375, 1309, 1255, 1039, 926, 746 cm^{-1}

1H NMR (400 MHz, $CDCl_3$) data:

δ 7.62 (dd, $J = 7.2, 1.8$ Hz, 1H), 7.36 (dd, $J = 7.9, 1.5$ Hz, 1H, H), 7.32 (td, $J = 7.1, 1.8$ Hz, 1H), 7.28 (td, $J = 7.1, 1.7$ Hz, 1H), 6.83 (d, $J = 1.4$ Hz, 1H), 6.79 (dd, $J = 8.0, 1.4$ Hz, 1H), 6.74 (d, $J = 7.8$ Hz, 1H) 6.51 (br s, 1H, D_2O exchangeable), 5.92 (s, 2H), 4.51 (d, $J = 5.6$ Hz, 2H)

^{13}C NMR (50 MHz, $CDCl_3$) data:

δ 168.3 (C), 147.9 (C), 147.0 (C), 134.8 (C), 131.4 (C), 131.3 (CH), 130.6 (C), 130.2 (CH), 130.1 (CH), 127.0 (CH), 121.2 (CH), 108.4 (CH), 108.3 (CH), 101.1 (CH_2), 44.0 (CH_2)

HR-ESI-MS: Positive mode: calcd. For $C_{15}H_{12}ClNO_3Na$ (m/z): 312.0421; found: 312.0398 ($[M + Na]^+$)

4.5.3. *N*-(3,4-Methylenedioxy)benzyl-2-iodobenzamide (3c)

White solid; m.p.: 141–142 °C

IR (KBr): 3253, 3067, 2992, 2899, 2841, 2779, 1969, 1929, 1848, 1637, 1539, 1503, 1443, 1251, 1036, 932, 806, 728 cm^{-1}

1H NMR (400 MHz, $CDCl_3$) data:

δ 7.83 (d, $J = 7.9$ Hz, 1H), 7.39–7.33 (m, 2H), 7.07 (td, $J = 7.5, 2.0$ Hz, 1H), 6.89 (d, $J = 1.2$ Hz, 1H), 6.83 (dd, $J = 7.9, 1.3$ Hz, 1H), 6.76 (d, $J = 7.9$ Hz, 1H), 5.97 (br s, 1H, D_2O exchangeable), 5.94 (s, 2H), 4.52 (d, $J = 5.6$ Hz, 2H).

^{13}C NMR (50 MHz, $CDCl_3$) data:

δ 169.1 (C), 147.9 (C), 147.1 (C), 141.9 (C), 139.9 (C), 131.3 (C), 131.2 (CH), 128.23 (CH), 128.16 (CH), 121.5 (CH), 108.7 (CH), 108.3 (CH), 101.1 (CH_2), 92.4 (C), 44.0 (CH_2)

HR-ESI-MS: Positive mode: calcd. For $C_{15}H_{12}INO_3Na$ (m/z): 403.9730; found: 403.9766 ($[M + Na]^+$)

4.5.4. *N*-(3,4-Methylenedioxy)benzyl-2-methylbenzamide (3d)

White solid; m.p.: 114–115 °C

IR (KBr): 3281, 3066, 3021, 2921, 2878, 2789, 1964, 1843, 1732, 1627, 1521, 1503, 1487, 1252, 1039, 933, 809, 741 cm^{-1}

1H NMR (400 MHz, $CDCl_3$) data:

δ 7.31 (d, $J = 7.6$ Hz, 1H), 7.27 (td, $J = 7.6, 1.1$ Hz, 1H), 7.19–7.13 (m, 2H), 6.81 (d, $J = 1.2$ Hz, 1H), 6.77 (dd, $J = 8.0, 1.2$ Hz, 1H), 6.74 (d, $J = 7.9$ Hz, 1H), 6.11 (br s, 1H, D_2O exchangeable), 5.92 (s, 2H), 4.47 (d, $J = 5.8$ Hz, 2H), 2.41 (s, 3H)

^{13}C NMR (50 MHz, $CDCl_3$) data:

δ 169.8 (C), 147.9 (C), 147.0 (C), 136.1 (C \times 2), 132.0 (C), 131.0 (CH), 129.9 (CH), 126.6 (CH), 125.7 (CH), 121.1 (CH), 108.35 (CH), 108.30 (CH), 101.0 (CH_2), 43.6 (CH_2), 19.8 (CH_3)

HR-ESI-MS: Positive mode: calcd. For $C_{16}H_{15}NO_3Na$ (m/z): 292.0944; found: 292.0966 ($[M + Na]^+$)

4.5.5. *N*-(3,4-Methylenedioxy)benzyl-2,6-difluorobenzamide (3e)

White solid; m.p.: 127–128 °C

IR (KBr): 3364, 3073, 3041, 3002, 2972, 2940, 2906, 2790, 1954, 1858, 1652, 1524, 1491, 1459, 1250, 1038, 999, 975, 926, 799, 776, 646 cm^{-1}

1H NMR (400 MHz, $CDCl_3$) data:

δ 7.34 (tt, $J = 8.4, 6.4$ Hz, 1H), 6.92 (*t*-like, $J = 8.2$ Hz, 1H), 6.84 (d, $J = 1.3$ Hz, 1H), 6.79 (dd, $J = 7.9, 1.3$ Hz, 1H), 6.75 (d, $J = 7.9$ Hz, 1H), 6.19 (br s, 1H, D_2O exchangeable), 5.93 (s, 2H), 4.54 (d, $J = 5.7$ Hz, 2H)

^{13}C NMR (50 MHz, $CDCl_3$) data:

δ 160.2 (C), 159.9 (dd, $J_{C-F} = 250.7, 6.5$ Hz, C), 147.9 (C), 147.1 (C), 131.7 (t, $J_{C-F} = 10.4$ Hz, C), 131.2 (C), 121.1 (CH), 114.1 (t, $J_{C-F} = 20.0$ Hz, CH), 112.0 (dd, $J_{C-F} = 22.7, 3.2$ Hz, CH), 108.3 (CH \times 2),

101.1 (CH_2), 43.8 (CH_2)

HR-ESI-MS: Positive mode: calcd. For $C_{15}H_{11}F_2NO_3Na$ (m/z): 314.0599; found: 314.0621 ($[M + Na]^+$)

4.5.6. *N*-(3,4-Methylenedioxy)benzyl-2-chloro-6-fluorobenzamide (3f)

White solid; m.p.: 114–115 °C

IR (KBr): 3260, 3069, 2911, 1848, 1648, 1544, 1489, 1445, 1254, 1040, 928, 899 cm^{-1}

1H NMR (400 MHz, $CDCl_3$) data:

δ 7.25 (td, $J = 8.2, 6.0$ Hz, 1H), 7.16 (br. d, $J = 8.0$ Hz, 2H), 6.99 (td, $J = 8.5, 0.9$ Hz, 1H), 6.82 (d, $J = 1.4$ Hz, 1H), 6.77 (dd, $J = 7.9, 1.4$ Hz, 1H), 6.73 (d, $J = 7.9$ Hz, 1H), 6.21 (br s, 1H, D_2O exchangeable), 5.91 (s, 2H, O- CH_2 -O), 4.51 (d, $J = 5.7$ Hz, 2H)

^{13}C NMR (50 MHz, $CDCl_3$) data:

δ 162.2 (C), 159.4 (d, $J_{C-F} = 251.5$ Hz, C), 147.9 (C), 147.0 (C), 132.3 (d, $J_{C-F} = 5.6$ Hz, C), 131.1 (d, $J_{C-F} = 9.4$ Hz, CH), 131.0 (C), 125.5 (d, $J_{C-F} = 4.0$ Hz, CH), 125.1 (d, $J_{C-F} = 21.6$ Hz, C), 121.2 (CH), 114.4 (d, $J_{C-F} = 22.3$ Hz, CH), 108.4 (CH), 108.3 (CH), 101.1 (CH_2), 43.8 (CH_2)

HR-ESI-MS: Positive mode: calcd. For $C_{15}H_{11}ClFNO_3Na$ (m/z): 330.0304; found: 330.0319 ($[M + Na]^+$)

4.5.7. *N*-(3,4-Methylenedioxy)benzyl-2-chloro-6-methylbenzamide (3g)

White solid; m.p.: 134–136 °C

IR (KBr): 3247, 3080, 2877, 2777, 1870, 1639, 1488, 1440, 1248, 1041, 944, 868 cm^{-1}

1H NMR (400 MHz, $CDCl_3$) data:

δ 7.17–7.15 (m, 2H), 7.07–7.05 (m, 1H), 6.85 (d, $J = 1.6$ Hz, 1H), 6.80 (dd, $J = 7.9, 1.6$ Hz, 1H), 6.74 (d, $J = 7.9$ Hz, 1H), 5.98 (br s, 1H, D_2O exchangeable), 5.93 (s, 2H), 4.53 (d, $J = 5.7$ Hz, 2H), 2.32 (s, 3H)

^{13}C NMR (50 MHz, $CDCl_3$) data:

δ 167.1 (C), 147.9 (C), 147.1 (C), 137.1 (C), 136.3 (C), 131.4 (C), 130.5 (CH), 129.8 (CH), 128.5 (CH), 126.7 (CH), 121.4 (CH), 108.6 (CH), 108.3 (CH), 101.1 (CH_2), 43.7 (CH_2), 19.3 (CH_3)

HR-ESI-MS: Positive mode: calcd. For $C_{16}H_{14}ClNO_3Na$ (m/z): 326.0544; found: 326.0578 ($[M + Na]^+$)

4.5.8. *N*-(3,4-Methylenedioxy)benzyl-2,6-dichlorobenzamide (Alda-1, 3 h)

White solid; m.p.: 175–176 °C

IR (KBr): 3258, 3072, 2930, 2899, 2871, 1850, 1641, 1549, 1486, 1430, 1248, 1217, 1039, 932, 789, 694 cm^{-1}

1H NMR (400 MHz, $CDCl_3$) data:

δ 7.31–7.29 (m, 2H), 7.25–7.21 (m, 1H), 6.89 (d, $J = 1.3$ Hz, 1H), 6.83 (dd, $J = 7.9, 1.3$ Hz, 1H), 6.75 (d, $J = 7.9$ Hz, 1H), 5.94 (s, 2H), 5.93 (br s, 1H, D_2O exchangeable), 4.57 (d, $J = 5.6$ Hz, 2H)

^{13}C NMR (100 MHz, $CDCl_3$) data:

δ 164.2 (C), 147.9 (C), 147.1 (C), 135.8 (C), 132.3 (C), 131.0 (C), 130.7 (CH), 128.1 (CH \times 2), 121.4 (CH), 113.8 (C), 108.6 (CH), 108.3 (CH), 101.1 (CH_2), 43.9 (CH_2)

HR-ESI-MS: Positive mode: calcd. For $C_{15}H_{11}Cl_2NO_3Na$ (m/z): 346.0008; found: 346.0024 ($[M + Na]^+$)

4.5.9. *N*-(3,4-Methylenedioxy)benzyl-2-hydroxybenzamide (3i)

White solid; m.p.: 125–126 °C

IR (KBr): 3365, 2923, 2853, 2786, 1851, 1726, 1637, 1590, 1547, 1499, 1484, 1442, 1378, 1353, 1303, 1253, 1231, 1192, 1148, 1122, 1078, 1042, 957, 939, 923, 867 cm^{-1}

1H NMR (200 MHz, $CDCl_3$) data:

δ 12.33 (br s, 1H, D_2O exchangeable), 7.39 (dd, $J = 8.6, 1.6$ Hz, 1H), 7.33 (ddd, $J = 9.7, 8.4, 1.4$ Hz, 1H), 6.98 (dd, $J = 8.4, 1.2$ Hz, 1H), 6.84–6.80 (m, 1H), 6.82–6.78 (m, 1H), 6.78 (dd, $J = 8.6, 1.3$ Hz, 1H), 6.77 (d, $J = 1.2$ Hz, 1H) 6.50 (br s, 1H, D_2O exchangeable), 5.94 (s, 2H), 4.51 (d, $J = 5.6$ Hz, 2H)

^{13}C NMR (50 MHz, $CDCl_3$) data:

δ 169.7 (C), 161.6 (C), 148.0 (C), 147.3 (C), 134.3 (CH), 133.3 (C), 131.7 (C), 131.1 (CH), 125.3 (CH), 121.3 (CH), 118.6 (CH), 114.0 (C),

108.4 (CH), 101.2 (CH₂), 43.5 (CH₂)

HR-ESI-MS: Positive mode: calcd. For C₁₅H₁₃NO₄Na (*m/z*): 294.0737; found: 294.0781 ([M + Na]⁺)

4.5.10. *N*-(3,4-Methylenedioxy)benzyl-2,6-dihydroxybenzamide (3j)

White solid; m.p.: 104–105 °C

IR (KBr): 3603, 3365, 3121, 2903, 1851, 1641, 1589, 1555, 1502, 1447, 1346, 1254, 1152, 1123, 1100, 1076, 1039, 1010, 979, 924, 863, 845, 806, 778, 762, 715, 637 cm⁻¹

¹H NMR (200 MHz, Methanol-*d*₄) data:

δ 7.13 (t, *J* = 8.3 Hz, 1H), 6.84 (d, *J* = 1.4 Hz, 1H), 6.82 (dd, *J* = 8.5, 1.4 Hz, 1H), 6.79 (d, *J* = 8.5 Hz, 1H), 6.35 (d, *J* = 8.3 Hz, 2H), 5.91 (s, 2H), 4.48 (s, 2H)

¹³C NMR (50 MHz, Methanol-*d*₄) data:

δ 171.7 (C), 161.6 (C), 149.3 (C), 148.2 (C), 134.4 (CH), 133.5 (C), 121.8 (CH), 109.1 (CH), 109.0 (CH), 108.4 (CH), 103.9 (C), 102.3 (C), 102.2 (CH₂), 43.6 (CH₂)

HR-ESI-MS: Positive mode: calcd. For C₁₅H₁₃NO₅Na (*m/z*): 310.0686; found: 310.0672 ([M + Na]⁺)

4.5.11. *N*-(3,4-Methylenedioxy)benzyl-2-bromobenzamide (3 k)

White solid; m.p.: 98–99 °C

IR (KBr): 3273, 3068, 2884, 2786, 1645, 1534, 1489, 1444, 1377, 1303, 1251, 1223, 1097, 1041, 928, 819 cm⁻¹

¹H NMR (400 MHz, CDCl₃) data:

δ 7.58–7.26 (m, 4H), 6.88–6.75 (m, 3H), 6.32 (br s, 1H, D₂O exchangeable), 5.95 (s, 2H), 4.53 (d, *J* = 5.6 Hz, 2H)

¹³C NMR (100 MHz, CDCl₃) data:

δ 167.4 (C), 147.9 (C), 147.0 (C), 137.5 (C), 133.3 (CH), 131.4 (C), 131.2 (CH), 129.5 (CH), 127.5 (CH), 121.3 (CH), 119.2 (C), 108.5 (CH), 108.3 (CH), 101.0 (CH₂), 41.0 (CH₂)

HR-ESI-MS: Positive mode: calcd. For C₁₅H₁₂BrNO₃Na (*m/z*): 355.9893; found: 355.9900 ([M + Na]⁺)

4.5.12. *N*-Benzyl-2,6-dichlorobenzamide (6a)

White crystal; 157–158 °C

IR (KBr): 3269, 3065, 3030, 2980, 2922, 2875, 1966, 1937, 1878, 1861, 1805, 1786, 1672, 1652, 1604, 1588, 1578, 1548, 1497, 1454, 1431, 1357, 1333, 1292, 1220, 1194, 1168, 1154, 1088, 1079, 1043, 1030, 957, 916, 800, 776, 761, 734, 698 cm⁻¹

¹H NMR (400 MHz, CDCl₃) data:

δ 7.38–7.19 (m, 8H), 6.5 (br s, 1H, D₂O exchangeable), 4.64 (d, *J* = 5.7 Hz, 2H)

¹³C NMR (100 MHz, CDCl₃) data:

δ 164.3 (C), 137.3 (C), 135.8 (C), 132.3 (C), 130.6 (CH), 128.7 (CH), 128.0 (CH), 128.0 (CH), 127.7 (CH), 44.0 (CH₂)

HR-ESI-MS: Positive mode: calcd. For C₁₄H₁₁NOCl₂Na (*m/z*): 302.0110; found: 302.0123 ([M + Na]⁺)

4.5.13. *N*-((4-Dimethylamino)benzyl)-2-chlorobenzamide (6c)

White solid; 122–123 °C

IR (KBr): 3262, 3066, 2914, 2875, 2793, 1960, 1925, 1889, 1859, 1812, 1620, 1593, 1524, 1435, 1349, 1312, 1188, 1128, 1058, 946, 792, 750, 725, 689, 580 cm⁻¹

¹H NMR (400 MHz, CDCl₃) data:

δ 7.65 (dd, *J* = 7.2, 2.0 Hz, 1H), 7.38–7.26 (m, 5H), 6.84 (br s, 2H), 6.36 (br s, 1H, D₂O exchangeable), 4.55 (d, *J* = 5.4 Hz, 2H), 2.95 (s, 6H)

¹³C NMR (100 MHz, CDCl₃) data:

δ 166.3 (C), 135.2 (C), 131.3 (C), 130.23 (C), 130.15 (CH), 129.2 (CH), 127.1 (CH), 43.9 (CH₂), 41.0 (CH₃)

HR-ESI-MS: Positive mode: calcd. For C₁₆H₁₇N₂OClNa (*m/z*): 311.0922; found: 311.0918 ([M + Na]⁺)

4.5.14. *N*-Isoamyl-2,6-dichlorobenzamide (6d)

White needle; m.p.: 112–113 °C

IR (KBr): 3274, 3091, 2955, 2924, 2867, 1667, 1644, 1586, 1557, 1454, 1430, 1385, 1341, 1298, 1192, 1172, 803, 786, 737, 695 cm⁻¹

¹H NMR (200 MHz, CDCl₃) data:

δ 7.29–7.16 (m, 3H), 5.80 (br s, 1H, D₂O exchangeable), 3.47 (dt, *J* = 7.3, 6.0 Hz, 2H), 1.68 (m, H-3'), 1.48 (q, *J* = 7.3 Hz, 2H), 0.93 (d, *J* = 6.5 Hz, 6H)

¹³C NMR (50 MHz, CDCl₃) data:

δ 164.4 (C), 136.2 (C), 132.2 (C), 130.5 (CH), 128.0 (CH), 38.2 (CH₂), 38.0 (CH₂), 25.7 (CH), 22.4 (CH₃),

HR-ESI-MS: Positive mode: calcd. For C₁₂H₁₅NOCl₂Na (*m/z*): 282.0423; found: 282.0440 ([M + Na]⁺)

4.5.15. *N*-(Thiophen-2-ylmethyl)-2-chlorobenzamide (6e)

Brown solid; m.p.: 84–85 °C

IR (KBr): 3275, 3049, 1640, 1592, 1529, 1468, 1450, 1430, 1367, 1294, 1258, 1158, 1126, 1061, 1036, 846, 833, 747, 703, 687 cm⁻¹

¹H NMR (400 MHz, CDCl₃) data:

δ 7.60 (dd, *J* = 7.2, 1.6 Hz, 1H), 7.39–7.22 (m, 4H), 7.04 (d, *J* = 3.2 Hz, 1H), 6.95 (dd, *J* = 5.0, 3.6 Hz, 1H), 6.55 (br s, 1H, D₂O exchangeable), 4.81 (d, *J* = 5.5 Hz, 2H)

¹³C NMR (100 MHz, CDCl₃) data:

δ 166.1 (C), 140.1 (C), 134.6 (C), 131.5 (CH), 130.7 (C), 130.27 (CH), 130.25 (CH), 127.1 (CH), 126.9 (CH), 126.3 (CH), 125.4 (CH), 38.9 (CH₂)

HR-ESI-MS: Positive mode: calcd. For C₁₂H₁₀NOSClNa (*m/z*): 274.0064; found: 274.0058 ([M + Na]⁺)

4.5.16. *N*-(2-chloro)benzyl-2,6-dichlorobenzamide (6f)

Orange solid; m.p.: 155–156 °C

IR (KBr): 3398, 1656, 1623, 1511, 1430, 1409, 1359, 1290, 1247, 1193, 1035, 986, 801, 758, 565 cm⁻¹

¹H NMR (400 MHz, CDCl₃) data:

δ 7.60–7.58 (m, 1H), 7.41–7.24 (m, 6H), 6.21 (br. s, 1H, D₂O exchangeable), 4.78 (d, *J* = 6.0, 2H)

¹³C NMR (100 MHz, CDCl₃) data:

δ 164.5 (C), 135.7 (C), 134.8 (C), 133.6 (C), 132.3 (CH), 130.7 (CH), 130.5 (C), 129.5 (CH), 129.2 (C), 128.1 (CH), 127.2 (CH), 41.9 (CH₂)

HR-ESI-MS: Positive mode: calcd. For C₁₄H₁₀NOCl₃Na (*m/z*): 335.9720; found: 335.9706 ([M + Na]⁺)

4.5.17. *N*-(3-Methoxy-4-hydroxy)benzyl-2-chlorobenzamide (6 g)

White solid; m.p.: 120–122 °C

IR (KBr): 3357, 3230, 2996, 2834, 1628, 1603, 1573, 1549, 1524, 1492, 1451, 1363, 1291, 1257, 1213, 1158, 1125, 1042, 987, 848, 813, 719 cm⁻¹

¹H NMR (400 MHz, Methanol-*d*₄) data:

δ 7.84–7.81 (m, 1H), 7.52–7.42 (m, 3H), 6.94 (d, *J* = 1.8, 1H), 6.81–6.73 (m, 2H), 4.47 (s, 2H), 3.82 (s, 3H)

¹³C NMR (100 MHz, Methanol-*d*₄) data:

δ 170.1 (C), 149.0 (C), 146.8 (C), 135.7 (C), 132.7 (CH), 131.3 (C), 129.6 (C), 129.6 (CH), 128.3 (CH), 121.4 (CH), 116.1 (CH), 112.5 (CH), 56.3 (CH₃), 44.4 (CH₂)

HR-ESI-MS: Positive mode: calcd. For C₁₅H₁₄NO₃ClNa (*m/z*): 314.0554; found: 314.0529 ([M + Na]⁺)

4.5.18. *N*-(3,4-Methylenedioxy)benzyl-3,3-dimethylacrylamide (8a)

White solid; m.p.: 57–58 °C

IR (KBr): 3278, 3168, 3063, 2973, 2939, 2907, 2795, 1848, 1671, 1624, 1484, 1493, 1361, 1281, 1250, 1229, 1179, 1102, 1040, 1016, 940, 924, 855, 818, 807, 672 cm⁻¹

¹H NMR (200 MHz, CDCl₃) data:

δ 6.90–6.86 (m, 2H), 6.86 (s, 1H, H-2'), 6.05 (s, 2H), 5.92 (br s, 1H, D₂O exchangeable), 5.69 (m, H-2), 4.47 (d, *J* = 5.2 Hz, 2H), 2.29 (d, *J* = 1.2 Hz, 3H), 1.95 (d, *J* = 1.2 Hz, 3H, 3-Me)

¹³C NMR (100 MHz, CDCl₃) data:

δ 166.7 (C), 151.1 (C), 147.6 (C), 146.6 (C), 132.5 (C), 120.8 (CH), 118.2 (CH), 108.2 (CH), 108.0 (CH), 100.8 (CH₂), 42.8 (CH₂), 27.0 (CH₃), 19.7 (CH₃)

HR-ESI-MS: Positive mode: calcd. For C₁₃H₁₅NO₃Na (*m/z*): 256.0944; found: 256.0973 ([M + Na]⁺)

4.5.19. *N*-(3,4-Methylenedioxy)benzyl-2-cyclopentylacetamide (8b)

White solid; m.p.: 110–112 °C

IR (KBr): 3248, 3071, 2959, 1649, 1629, 1556, 1505, 1444, 1252, 1212, 1039, 926, 811, 645 cm⁻¹

¹H NMR (400 MHz, CDCl₃) data:

δ 6.73–6.70 (m, 3H), 5.91 (s, 2H), 5.79 (br s, 1H, D₂O exchangeable), 4.31 (d, *J* = 5.6 Hz, 2H), 2.22–2.17 (m, 3H), 1.86–1.76 (m, 2H), 1.62–1.49 (m, 4H), 1.17–1.07 (m, 2H)

¹³C NMR (100 MHz, CDCl₃) data:

δ 172.8 (C), 148.0 (C), 147.0 (C), 132.3 (C), 121.1 (CH), 108.5 (CH), 108.4 (CH), 101.1 (CH₂), 43.5 (CH₂), 43.1 (CH₂), 37.2 (CH), 32.6 (CH₂), 25.0 (CH₂)

HR-ESI-MS: Positive mode: calcd. For C₁₅H₁₉NO₃Na (*m/z*): 284.1257; found: 284.1251 ([M + Na]⁺)

4.5.20. *N*-(3,4-Methylenedioxy)benzylbutyramide (8c)

Pale yellow solid; m.p.: 58–60 °C

IR (KBr): 3248, 3071, 2959, 1649, 1629, 1556, 1505, 1444, 1252, 1212, 1039, 926, 811, 645 cm⁻¹

¹H NMR (400 MHz, Methanol-*d*₄) data:

δ 6.76–6.73 (m, 3H), 5.90 (s, 3H), 4.24 (s, 2H), 2.18 (t, *J* = 7.2, 2H), 1.63 (sextet, *J* = 7.5 Hz, 2H), 0.93 (t, *J* = 7.4 Hz, 3H)

¹³C NMR (100 MHz, Methanol-*d*₄) data:

δ 174.5 (C), 147.9 (C), 146.9 (C), 132.7 (C), 120.6 (CH), 107.8 (CH), 107.7 (CH), 101.0 (CH₂), 42.5 (CH₂), 37.7 (CH₂), 19.1 (CH₂), 12.6 (CH₃)

HR-ESI-MS: Positive mode: calcd. For C₁₂H₁₅NO₃Na (*m/z*): 244.0944; found: 244.0936 ([M + Na]⁺)

4.5.21. *N*-(2,6-Dichloro)benzyl-(3,4-methylenedioxy)benzamide (11a)

White solid; m.p.: 172–173 °C

IR (KBr): 3317, 3092, 3068, 3002, 2963, 2913, 2464, 2414, 1942, 1870, 1789, 1744, 1635, 1614, 1504, 1437, 1421, 1350, 1250, 1039, 930, 874, 764 cm⁻¹

¹H NMR (200 MHz, CDCl₃) data:

δ 7.38–7.14 (m, 5H), 6.78 (d, *J* = 8.7 Hz, 1H), 6.30 (br. s, 1H, D₂O exchangeable), 5.99 (s, 2H), 4.91 (d, *J* = 5.4 Hz, 2H)

¹³C NMR (50 MHz, CDCl₃) data:

δ 166.3 (C), 150.3 (C), 147.9 (C), 136.2 (C × 2), 133.5 (C), 129.6 (CH), 128.5 (CH × 2), 128.3 (C), 121.6 (CH), 107.9 (CH), 107.7 (CH), 101.6 (CH₂), 39.8 (CH₂)

HR-ESI-MS: Positive mode: calcd. For C₁₅H₁₁NO₃Cl₂Na (*m/z*): 346.0008; found: 346.0022 ([M + Na]⁺)

4.5.22. *N*-2-Chlorobenzyl-(3,4-methylenedioxy)benzamide (11b)

White solid; m.p.: 109–110 °C

IR (KBr): 3304, 3065, 2895, 2789, 2456, 2364, 1845, 1634, 1617, 1603, 1546, 1458, 1354, 1308, 1259, 1040, 937, 750, 600, 522 cm⁻¹

¹H NMR (400 MHz, CDCl₃) data:

δ 7.42–7.15 (m, 6H), 6.77 (d, *J* = 7.9 Hz, 1H), 6.65 (br. s, 1H, D₂O exchangeable), 5.98 (s, 2H), 4.64 (d, *J* = 5.6 Hz, 2H)

¹³C NMR (50 MHz, CDCl₃) data:

δ 166.7 (C), 150.4 (C), 147.9 (C), 135.5 (C), 133.6 (C), 130.2 (CH), 129.5 (CH), 128.9 (CH), 128.3 (C), 127.1 (CH), 121.6 (CH), 107.9 (CH), 107.6 (CH), 101.7 (CH₂), 42.0 (CH₂)

HR-ESI-MS: Positive mode: calcd. For C₁₅H₁₂NO₃ClNa (*m/z*): 312.0398; found: 312.0414 ([M + Na]⁺)

4.5.23. *N*-(2,6-Difluoro)benzyl-(3,4-methylenedioxy)benzamide (11c)

White solid; m.p.: 129–130 °C

IR (KBr): 3338, 3279, 3075, 2996, 2944, 2910, 2786, 2478, 2416, 1926, 1865, 1761, 1635, 1624, 1603, 1550, 1502, 1457, 1419, 1358, 1260, 1061, 1034, 981, 883, 821, 787, 760, 490 cm⁻¹

¹H NMR (400 MHz, CDCl₃) data:

δ 7.27–7.20 (m, 3H), 6.88 (t, *J* = 7.9 Hz, 2H), 6.77 (d, *J* = 8.0 Hz, 1H), 6.44 (br. s, 1H, D₂O exchangeable), 5.98 (s, 2H), 4.69 (d, *J* = 5.6 Hz, 2H)

¹³C NMR (100 MHz, CDCl₃) data:

δ 166.3 (C), 161.5 (dd, *J*_{C-F} = 247.4, 8.0, C), 150.3 (C), 147.9 (C), 129.5 (t, *J*_{C-F} = 10.3, CH), 128.3 (CH), 121.6 (CH), 113.8 (t, *J*_{C-F} = 19.1 Hz, C), 111.4 (dd, *J*_{C-F} = 18.8, 6.6 Hz, CH), 107.9 (CH), 107.7 (CH), 101.6 (CH₂), 32.0 (t, *J*_{C-F} = 3.7 Hz, CH₂)

HR-ESI-MS: Positive mode: calcd. For C₁₅H₁₁NO₃F₂Na (*m/z*): 314.0599; found: 314.0624 ([M + Na]⁺)

4.5.24. *N*-(2,6-Dichloro)benzyl-3,4-methylenedioxy-5-hydroxybenzamide (11d)

White solid; m.p.: 163 °C decomposed

IR (KBr): 3444, 3287, 1937, 1781, 1552, 1459, 1437, 1405, 1390, 1309, 1260, 1220, 1177, 1111, 1074, 1043, 1025, 929, 778, 715, 649 cm⁻¹

¹H NMR (400 MHz, Methanol-*d*₄) data:

δ 7.41–7.26 (m, 3H), 6.87 (d, *J* = 1.6 Hz, 1H), 6.73 (d, *J* = 1.7 Hz, 1H), 5.91 (s, 2H), 4.79 (s, 2H)

¹³C NMR (100 MHz, Methanol-*d*₄) data:

δ 170.2 (C), 150.0 (C), 145.4 (C), 139.4 (C), 137.6 (C), 134.4 (C), 131.0 (CH), 129.7 (CH), 129.3 (C), 114.1 (CH), 102.5 (CH₂), 99.3 (CH), 41.0 (CH₂)

HR-ESI-MS: Positive mode: calcd. For C₁₅H₁₁NO₄Cl₂Na (*m/z*): 361.9957; found: 361.9970 ([M + Na]⁺)

4.5.25. *N*-(2,6-Dichloro)benzyl-3,4-methylenedioxy-5-methoxybenzamide (11e)

White solid; m.p.: 178–179 °C

IR (KBr): 3259, 3082, 2940, 2896, 1719, 1620, 1547, 1505, 1462, 1437, 1426, 1366, 1320, 1236, 1192, 1120, 1091, 1038, 925, 862, 779, 767, 664 cm⁻¹

¹H NMR (400 MHz, CDCl₃) data:

δ 7.37–7.20 (m, 3H), 7.15 (d, *J* = 1.5 Hz, 1H), 6.86 (d, *J* = 1.5 Hz, 1H), 6.38 (br s, 1H, D₂O exchangeable), 6.04 (s, 2H), 4.94 (d, *J* = 5.5 Hz, 2H), 3.93 (s, 3H)

¹³C NMR (100 MHz, CDCl₃) data:

δ 166.2 (C), 149.3 (C), 148.7 (C), 143.5 (C), 138.1 (C), 136.2 (C), 133.4 (C), 129.6 (CH), 128.5 (CH), 108.1 (CH), 102.1 (CH₂), 100.7 (CH), 56.6 (CH₃), 39.8 (CH₂)

HR-ESI-MS: Positive mode: calcd. For C₁₆H₁₃NO₄Cl₂Na (*m/z*): 376.0114; found: 376.0118 ([M + Na]⁺)

4.5.26. *N*-(2,6-Dichloro)benzyl-3,4-methylenedioxy-cinnamic amide (22)

White solid; m.p.: 157–158 °C

IR (KBr): 3274, 2923, 2851, 1647, 1614, 1533, 1497, 1444, 1376, 1245, 1190, 1102, 1040, 1020, 969, 935, 848, 813, 783, 766 cm⁻¹

¹H NMR (200 MHz, CDCl₃) data:

δ 7.57 (d, *J* = 15.5 Hz, 1H), 7.36–7.14 (m, 3H), 6.98 (d, *J* = 1.9 Hz, 1H), 6.96 (dd, *J* = 8.5, 1.5 Hz, 1H), 6.78 (d, *J* = 8.5 Hz, 1H), 6.20 (d, *J* = 15.5 Hz, 1H), 5.98 (s, 2H), 4.88 (d, *J* = 5.5, 2H)

¹³C NMR (50 MHz, CDCl₃) data:

δ 165.5 (C), 149.1 (C), 148.2 (C), 135.1 (C), 134.9 (C), 133.5 (C), 131.2 (C), 129.6 (CH), 128.5 (CH), 124.4 (CH), 124. (CH), 124.2 (CH), 118.0 (CH), 108.5 (CH), 106.3 (CH), 101.4 (CH₂), 40.1 (CH₂)

HR-ESI-MS: Positive mode: calcd. For C₁₇H₁₃NO₃Cl₂Na (*m/z*): 372.0165; found: 372.0178 ([M + Na]⁺)

4.5.27. *N*-Piperonyl-*N*-methyl-2-chlorobenzamide (27a)

Yellow oil

IR (KBr): 1735, 1638, 1502, 1490, 1444, 1402, 1292, 1244, 1188,

1085, 1039, 928, 770, 748 cm^{-1}

^1H NMR (400 MHz, CDCl_3) data:

Form A: δ 7.34–7.20 (m, 4H), 6.85–6.52 (m, 3H), 5.88 (s, 2H), 4.77–4.45 (m, 2H), 2.65 (s, 3H)

Form B: δ 7.34–7.20 (m, 4H), 6.85–6.52 (m, 3H), 5.87 (s, 2H), 4.30–4.10 (m, 2H), 2.94 (s, 3H)

^{13}C NMR (100 MHz, CDCl_3) data:

δ 168.60 (C), 168.56 (C), 148.1 (C), 148.0 (C), 147.1 (C), 136.2 (C), 136.0 (C), 130.5 (CH), 130.4 (CH), 130.2 (CH), 130.1 (CH), 129.8 (CH), 129.7 (CH), 129.65 (C), 128.0 (CH), 127.7 (CH), 127.23 (CH), 127.20 (CH), 121.8 (C), 120.8 (C), 108.8 (C), 108.4 (C), 108.2 (CH), 107.6 (CH), 101.2 (CH_2), 101.1 (CH_2), 54.2 (CH_2), 50.1 (CH_2), 35.2 (CH_3), 32.1 (CH_3)

HR-ESI-MS: Positive mode: calcd. For $\text{C}_{16}\text{H}_{14}\text{NO}_3\text{ClNa}$ (m/z): 326.0544; found: 326.0540 ($[\text{M} + \text{Na}]^+$)

4.5.28. *N*-Piperonyl-*N*-isopropyl-2-chlorobenzamide (27b)

Yellow solid; m.p.: 132–134 °C

IR (KBr): 1631, 1571, 1502, 1490, 1390, 1258, 1244, 1148, 1048, 941, 808, 760, 647 cm^{-1}

^1H NMR (400 MHz, CDCl_3) data:

δ 7.53–7.52 (m, 1H), 7.33–7.30 (m, 1H), 7.21–7.18 (m, 2H), 7.03 (s, 1H), 6.89 (dd, $J = 7.9, 0.9$ Hz, 1H), 6.64 (d, $J = 7.9$ Hz, 1H), 5.83 (s, 2H), 3.84 (s, 2H), 3.13, (sept, $J = 6.4$ Hz, 1H), 1.22 (d, $J = 6.2$ Hz, 6H)

^{13}C NMR (100 MHz, CDCl_3) data:

δ 172.2 (C), 147.9 (C), 147.8 (C), 139.3 (C), 130.8 (C), 129.9 (CH), 129.2 (CH), 126.4 (CH), 125.2 (CH), 124.2 (CH), 110.7 (CH), 108.3 (CH), 101.2 (CH_2), 48.4 (CH_2), 47.8 (CH), 18.9 (CH_3)

HR-ESI-MS: Positive mode: calcd. For $\text{C}_{18}\text{H}_{18}\text{NO}_3\text{ClNa}$ (m/z): 354.0867; found: 354.0870 ($[\text{M} + \text{Na}]^+$)

4.5.29. 3-(3,4-Methylenedioxy)phenyl-5-propyl-1,2,4-oxadiazole (29b)

White solid; m.p.: 39–40 °C

IR (KBr): 2966, 1868, 1800, 1729, 1631, 1579, 1531, 1453, 1389, 1334, 1258, 1238, 1164, 1112, 1038, 937, 880, 821, 745 cm^{-1}

^1H NMR (400 MHz, CDCl_3) data:

δ 7.60 (dd, $J = 8.1, 1.6$ Hz, 1H), 7.49 (d, $J = 1.6$ Hz, 1H), 6.87 (d, $J = 8.1$ Hz, 1H), 6.00 (s, 2H), 2.87 (t, $J = 7.4$ Hz, 2H), 1.87 (sextet, $J = 7.4$ Hz, 2H), 1.03 (t, $J = 7.4$ Hz, 3H)

^{13}C NMR (100 MHz, CDCl_3) data:

δ 179.6 (C), 167.9 (C), 150.0 (C), 148.0 (C), 122.2 (CH), 120.8 (C), 108.6 (CH), 107.4 (CH), 101.5 (CH_2), 28.4 (CH_2), 20.2 (CH_2), 13.6 (CH_3)

HR-ESI-MS: Positive mode: calcd. For $\text{C}_{12}\text{H}_{12}\text{N}_2\text{O}_3\text{Na}$ (m/z): 255.0740; found: 255.0721 ($[\text{M} + \text{Na}]^+$)

4.5.30. 7-Methoxyisoflavone (33a)

White solid; m.p.: 137–138 °C

IR (KBr): 3074, 3021, 2924, 1633, 1600, 1567, 1500, 1483, 1367, 1329, 1290, 1204, 1098, 1052, 1027, 968, 941, 884, 823, 787, 722, 662, 529 cm^{-1}

^1H NMR (400 MHz, CDCl_3) data:

δ 8.19 (d, $J = 8.9$ Hz, 1H), 7.92 (s, 1H), 7.53 (dd, $J = 8.3, 1.3$ Hz, 2H), 7.43–7.34 (m, 3H), 6.97 (dd, $J = 8.9, 2.2$ Hz, 1H), 6.83 (d, $J = 2.2$ Hz, 1H), 3.88 (s, 3H)

^{13}C NMR (100 MHz, CDCl_3) data:

δ 175.7 (C), 164.1 (C), 159.0 (C), 152.7 (CH), 132.0 (C), 129.1 (CH), 128.5 (CH), 128.2 (CH), 127.9 (CH), 125.3 (C), 118.5 (C), 114.7 (CH), 100.2 (CH), 55.9 (CH_3)

HR-ESI-MS: Positive mode: calcd. For $\text{C}_{16}\text{H}_{12}\text{O}_3\text{Na}$ (m/z): 275.0679; found: 275.0664 ($[\text{M} + \text{Na}]^+$)

4.5.31. Isoformononetin (33b)

White solid; m.p.: 208–210 °C

IR (KBr): 3215, 3054, 2852, 2362, 1723, 1622, 1586, 1515, 1441, 1379, 1255, 1172, 1098, 1018, 942, 831, 796, 779, 698, 542 cm^{-1}

^1H NMR (400 MHz, CDCl_3) data:

δ 9.37 (br s, 1H, D_2O exchangeable), 8.11 (d, $J = 8.9$ Hz, 1H), 8.01 (s, 1H), 7.41 (d, $J = 8.4$ Hz, 2H), 7.02 (dd, $J = 8.9$ Hz, 1.2, 1H), 7.01 (d, $J = 1.2$ Hz, 1H), 6.87 (d, $J = 8.4$ Hz, 2H), 3.95 (s, 3H)

^{13}C NMR (100 MHz, CDCl_3) data:

δ 174.3 (C), 163.0 (C), 156.7 (C), 156.6 (CH), 151.0 (C), 128.7 (CH), 125.8 (CH), 123.2 (CH), 121.3 (CH), 116.5 (C), 113.8 (CH), 98.9 (CH), 54.4 (CH_3)

HR-ESI-MS: Positive mode: calcd. For $\text{C}_{16}\text{H}_{12}\text{O}_4\text{Na}$ (m/z): 291.0628; found: 291.0630 ($[\text{M} + \text{Na}]^+$)

4.5.32. 3-(4-Pyridinyl)-7-methoxychromone (33c)

Yellow solid; m.p.: 152–153 °C

IR (KBr): 3219, 3054, 2920, 2851, 1638, 1600, 1506, 1445, 1382, 1322, 1271, 1098, 1053, 942, 892, 824, 796, 779, 696, 540 cm^{-1}

^1H NMR (400 MHz, CDCl_3) data:

δ 8.66 (dd, $J = 4.5, 1.6$ Hz, 2H), 8.20 (d, $J = 8.9$ Hz, 1H), 8.07 (s, 1H), 7.63 (dd, $J = 4.6, 1.6$ Hz, 2H), 7.02 (dd, $J = 8.9, 2.3$ Hz, 1H), 6.88 (d, $J = 2.3$ Hz, 1H), 3.92 (s, 3H)

^{13}C NMR (50 MHz, CDCl_3) data:

δ 174.7 (C), 164.4 (C), 157.8 (C), 153.5 (CH), 150.6 (C), 149.6 (CH), 127.8 (CH), 123.3 (CH), 121.4 (CH), 118.2 (C), 115.1 (CH), 100.2 (CH), 55.9 (CH_3)

HR-ESI-MS: Positive mode: calcd. For $\text{C}_{15}\text{H}_{12}\text{NO}_3$ (m/z): 254.0812; found: 254.0828 ($[\text{M} + \text{H}]^+$) calcd. For $\text{C}_{15}\text{H}_{11}\text{NO}_3\text{Na}$ (m/z): 276.0631; found: 276.0663 ($[\text{M} + \text{Na}]^+$)

Declaration of Competing Interest

The authors declare that they have no known competing financial interests or personal relationships that could have appeared to influence the work reported in this paper.

Appendix A. Supplementary material

Supplementary data to this article can be found online at <https://doi.org/10.1016/j.bioorg.2020.104166>.

References

- [1] M.Y. Eng, S.E. Luczak, T.L. Wall, Alcohol Res. Health 30 (2007) 22–27.
- [2] V. Bagnardi, M. Rota, E. Botteri, I. Tramacere, F. Islami, V. Fedirko, L. Scotti, M. Jenab, F. Turati, E. Pasquali, Br. J. Cancer 112 (2015) 580–593.
- [3] M.-F. Wang, C.-L. Han, S.-J. Yin, Chem. Biol. Interact. 178 (2009) 36–39.
- [4] A.I. Cederbaum, Clin. Liver Dis. 16 (2012) 667–685.
- [5] C.H. Chen, J.C. Ferreira, E.R. Gross, D. Mochly-Rosen, Physiol. Rev. 94 (2014) 1–34.
- [6] Li, H.; Borinskaya, S.; Yoshimura, K.; Kal'ina, N.; Marusin, A.; Stepanov, V. A.; Qin, Z.; Khaliq, S.; Lee, M. Y.; Yang, Y. Ann. Hum. Genet. 73 (2009) 335–345.
- [7] C.H. Chen, G.R. Budas, E.N. Churchill, M.H. Disatnik, T.D. Hurley, D. Mochly-Rosen, Science 321 (2008) 1493–1495.
- [8] R.-L. Yu, C.-H. Tan, Y.-C. Lu, R.-M. Wu, Sci. Rep. 6 (2016) 30424.
- [9] J.S. Chang, J.-R. Hsiao, C.-H. Chen, J. Biomed. Sci. 24 (2017) 19.
- [10] E.R. Gross, V.O. Zambelli, B.A. Small, J.C. Ferreira, C.H. Chen, D. Mochly-Rosen, Annu. Rev. Pharmacol. Toxicol. 55 (2015) 107–127.
- [11] S. Perez-Miller, H. Younus, R. Vanam, C.-H. Chen, D. Mochly-Rosen, T.D. Hurley, Nat. Struct. Mol. Biol. 17 (2010) 159–164.
- [12] H.N. Larson, J. Zhou, Z. Chen, J.S. Stamler, H. Weiner, T.D. Hurley, J. Biol. Chem. 282 (2007) 12940–12950.
- [13] H.N. Larson, H. Weiner, T.D. Hurley, J. Biol. Chem. 280 (2005) 30550–30556.
- [14] C.G. Steinmetz, P. Xie, H. Weiner, T.D. Hurley, Structure 5 (1997) 701–711.
- [15] J.-M. Guo, A.-J. Liu, P. Zang, W.-Z. Dong, L. Ying, W. Wang, P. Xu, X.-R. Song, J. Cai, S.-Q. Zhang, J.-L. Duan, J.L. Mehta, D.-F. Su, Cell Res. 23 (2013) 915–930.
- [16] K. Matsuo, I. Oze, S. Hosono, H. Ito, M. Watanabe, K. Ishioka, S. Ito, M. Tajika, Y. Yatabe, Y. Niwa, K. Yamao, S. Nakamura, K. Tajima, H. Tanaka, Carcinogenesis 34 (2013) 1510–1515.
- [17] W. Wang, L.-L. Lin, J.-M. Guo, Y.-Q. Cheng, J. Qian, J.L. Mehta, D.-F. Su, P. Luan, A.-J. Liu, Int. J. Stroke 10 (2015) 1261–1269.
- [18] T. Zhang, Q. Zhao, F. Ye, C. Huang, W.-M. Chen, W.-Q. Huang, Free Radic. Res. 52 (2018) 629–638.
- [19] D. Mochly-Rosen, C.H. Chen, W.J. Yang, WO patent NO. 2010062308 (2010).
- [20] S. Talukdar, J.-L. Hsu, T.-C. Chou, J.-M. Fang, Tetrahedron Lett. 42 (2001) 1103–1105.

- [21] A.H. Rezvani, D.H. Overstreet, M. Perfumi, M. Massi, *Pharmacol. Biochem. Behav.* 75 (2003) 593–606.
- [22] K. WingMing, B.L. Vallee, *Phytochemistry* 47 (1998) 499–506.
- [23] V. Koppaka, D.C. Thompson, Y. Chen, M. Ellermann, K.C. Nicolaou, R.O. Juvonen, D. Petersen, R.A. Deitrich, T.D. Hurley, V. Vasilou, *Pharmacol. Rev.* 64 (2012) 520–539.
- [24] M. Mangold, L. Rolland, F. Costanzo, M. Sprik, M. Sulpizi, J. Blumberger, *J. Chem. Theory Comput.* 7 (2011) 1951–1961.
- [25] K.F. Biegasiewicz, J.S. Gordon, D.A. Rodriguez, R. Priefer, *Tetrahedron Lett.* 55 (2014) 5210–5212.
- [26] G. Cavallo, P. Metrangolo, R. Milani, T. Pilati, A. Priimagi, G. Resnati, G. Terraneo, *Chem. Rev.* 116 (2016) 2478–2601.
- [27] E.D. Lowe, G.-Y. Gao, L.N. Johnson, W.M. Keung, *J. Med. Chem.* 51 (2008) 4482–4487.